MODIFICATION OF MEMBRANES BY INCORPORATING TIO_2-GRAPHENE OXIDE FOR ENHANCED WATER PURIFICATION PERFORMANCE

BY

ANWAR QASEM AL GAMAL

A Thesis Presented to the

DEANSHIP OF GRADUATE STUDIES

KING FAHD UNIVERSITY OF PETROLEUM & MINERALS

DHAHRAN, SAUDI ARABIA

In Partial Fulfillment of the
Requirements for the Degree of

MASTER OF SCIENCE

In

MECHANICAL ENGINEERING

APRIL 2021

MODIFICATION OF MEMBRANES BY INCORPORATING TiO_2-GRAPHENE OXIDE FOR ENHANCED WATER PURIFICATION PERFORMANCE

Anwar Qasem Ahmed Al Gamal

MECHANICAL ENGINEERING

APRIL 2021

KING FAHD UNIVERSITY OF PETROLEUM & MINERALS

DHAHRAN- 31261, SAUDI ARABIA

DEANSHIP OF GRADUATE STUDIES

This thesis, written by **Anwar Qasem Ahmed Al Gamal** under the direction of his thesis advisor and approved by his thesis committee, has been presented and accepted by the Dean of Graduate Studies, in partial fulfillment of the requirements for the degree of **MASTER OF SCIENCE IN MECHANICAL ENGINEERING.**

Dr. Wail S. Falath
(Advisor)

PP. Almerbad.

Dr. Khaled S. Al-Athel
Department Chairman

Dr. Khaled Mezghani
(Member)

Dr. Soliman S. Al-Homidan
Dean of Graduate Studies

Dr. Tawfik A. Saleh
(Member)

Date

This thesis is *dedicated to my beloved parents for their limitless support*

ACKNOWLEDGMENTS

All praise and glorifications to ALLAH (S. W. T), who created the chance and provided me with health, patience, and guidance to accomplish my MS degree at King Fahd University of Petroleum and Minerals (KFUPM), Saudi Arabia. KFUPM and Center for Environment and Water are gratefully thanked for their funding and supporting during this research. Mechanical engineering department, Chemistry department, Physics department, Centre of Excellence in Nano Technology and Center for Environment and Water are also acknowledged for supplying the required facilities to perform the experimental work.

I would firstly like to express my great thanks to my thesis advisor Dr. Wail S. Falath, for all of his help, support, encouragement, continuous motivation and guidance during the whole work. I would like also to thank and acknowledge my committee members Dr. Tawfik A. Saleh and Dr. Khaled Mezghani for their friendly discussion, continuous encouragement and valuable advice. Sincere thanks are to all of my colleagues and friends at KFUPM especially graduate students that I have interacted with them during my research work.

Above all, sincere thanks are to my father who passed away recently, and my mother, for their endless inspiration, encouragement, love, assistance and incessant prayers throughout my life. I would like also to offer my great thankfulness to my wife, brothers and sisters for their love, encouragement, and constant assistance during my research work.

TABLE OF CONTENTS

LIST OF TABLES

LIST OF FIGURES

LIST OF ABBREVIATIONS

AFM	:	Atomic Force Microscopy
CA	:	Contact Angle
DI	:	Deionized Water
EDX	:	Energy-Dispersive X-ray
ED	:	Electrodialysis
FT-IR	:	Fourier Transformation Infrared
GO	:	Graphene Oxide
IC	:	Ion Chromatography
P	:	Polymerization
J	:	Permeate Flux
LMH	:	Flux Unit
MED	:	Multiple-Effect Distillation
MPD	:	m-Phenylenediamine
MSF	:	Multi-Stage Flash
MWNTs	:	Multi-Walled Carbon Nanotubes
PA	:	Polyamide

PSf	:	Polysulfone
R	:	Salt Rejection
RO	:	Reverse Osmosis
RMS	:	Root Mean Square Roughness
SEM	:	Scanning Electron Microscope
TFC	:	Thin-Film Composite
TiO_2	:	Titanium Dioxide
TMC	:	Trimesoyl Chloride
VC	:	Vapor Compression
XPS	:	X-ray Photoelectron Spectroscopy
XRD	:	X-Ray Diffraction

ABSTRACT

Full Name : [Anwar Qasem Al Gamal]

Thesis Title : [Modification of Membranes by Incorporating TiO2 -Graphene Oxide for Enhanced Water Purification Performance]

Major Field : [Mechanical Engineering]

Date of Degree : [April 2021]

Membrane-based separation processes are very effective for several applications such as purification of drinking water and treatment of wastewater. They have a huge potential to enhance the desalination efficiency of seawater with efficient cost and energy requirements. Therefore, they have received great interest around the world. Polymer-inorganic composite reverse osmosis membrane is a powerful method that opens the door to merge different properties of inorganic materials like mechanical and thermal stability with organic polymer properties including processability and flexibility in one solid. The aim of this work is to modify aromatic polyamide membrane surfaces by the simultaneous incorporation of graphene oxide (GO) and TiO_2 nanoparticles, for enhancing the salt rejection and filtration performance of the membrane. The 1, 3, 5-benzenetricarbonyl chloride (TMC), TiO_2-GO compound, and m-phenylenediamine (MPD) were prepared and polymerized on the surface of a porous support layer made of polysulfone (PSf). The TiO_2-GO compound was mixed with MPD aqueous solution because its dispersion in aqueous solution was stronger than in organic solvents. Fourier Transform Infra-Red (FTIR) spectroscopy, X-ray Photoelectron Spectroscopy (XPS), and X-ray Diffraction (XRD) were applied to confirm the presence of TiO_2-GO compound on

the membrane surface. Scanning Electron Microscopy (SEM) equipped with Energy-Dispersive X-ray (EDX), and Atomic Force Microscopy (AFM) were carried out to analyze the surface morphology and reveal the smoothening of the modified membrane surface. Water contact angle measurements were carried out to visualize the hydrophilicity improvements of modified membranes. The performance parameters of the membrane including permeate flux, salt rejection, and hydrocarbons rejection were evaluated using a custom-made laboratory setup. The incorporation of TiO_2-GO compound into the membrane matrix enhanced the membrane performance with 62 LMH (Lm^{-2} h^{-1}) permeate flux, 97 % salt rejection, and 100 % hydrocarbons rejection, due to changes in charge, roughness, and hydrophilicity of the membrane surface.

ملخص الرسالة

الاسم الكامل: أنور قاسم الجمل

عنوان الرسالة: تعديل الأغشية بدمج ثاني أكسيد التيتانيوم مع أكسيد الجرافيين لتحسين أداء تنقية المياة

التخصص: الهندسة الميكانيكية

تاريخ الدرجة العلمية: أبريل 2021

إن عمليات الفصل المعتمدة على الأغشية فعالة جداً للعديد من التطبيقات مثل : تنقية مياة الشرب ومعالجة مياة الصرف، فهذه العمليات تمتلك إمكانية عالية في تحسين فعالية تحلية مياة البحر بسعر وطاقة مناسبين. لذالك أكتسبت أهتمام كبير من قبل العلماء و الباحثين على مستوى العالم. فغشاء التناضح العكسي المكون من بوليمر وجزيئات غير عضوية أسلوب قوي فتحَ آفاق جديدة لدمج الخصائص المختلفة للمواد الغير عضوية مثل الثبات الحراري والميكانيكي مع خصائص البوليمرات العضوية مثل قابلية المعالجة والمرونة في مركب واحد.

الهدف من هذه الرسالة هو تعديل وتطوير غشاء تناضح عكسي مصنوع من مادة البولي أميد الحلقي عن طريق دمج جزيئات أكسيد الجرافين وثاني أكسيد التيتانيوم معا على سطحه لتحسين أداء الغشاء في فصل الملح وتنقية المياة. تم تصنيع هذه الأغشية عن طريق تحضير محلول من مادة كلوريد التريمسويل ومحلول من مادة م- فينيلين ديامين مضاف إليه مادتي أكسيد الجرافين وثاني أكسيد التيتانيوم وتم مزجهم على سطح طبقة رقيقة مصنوعة من مادة البولي سلفون بواسطة البلمرة السطحية. عند مزج المحاليل المختلفة تم مراعاة مزج مركب مادة أكسيد الجرافين وثاني أكسيد التيتانيوم مع ملحول م- فينيلين ديامين كون هذه المادة تبددُ وتذوبُ بشكل فعال في الماء مقارنة بالمذيبات العضوية.

تم قياس وتوصيف وأثبات أضافة مركب أكسيد الجرافين وثاني أكسيد التيتانيوم الى الأغشية المحضرة عن طريق تقنيات عدة مثل مقياس طيف الأشعة تحت الحمراء،مطياف الأشعة السينية الإلكترونية الضوئية، وحيود الأشعة السينية. بالأضافة إلى ذالك، أستخدمت تقنيات أخرى مثل: مجهر المسح الإلكتروني مع مطيافية تشتت الطاقة بالأشعة السينية،ومجهر القوة الذرية لدراسة وتحليل شكل ومظهر وخشونة أسطح الأغشية بعد تعديلها. كما

أُستخدمت قياسات زاوية ملامسة الماء لأسطح الأغشية لدراسة وتحليل قابلية سطح الغشاء بعد التعديل للاتحاد مع الماء.كما تم قياس ومعايينة كفاءة الغشاء المعدل في فصل الملح والزيت من الماء بواسطة نظام مصنوع بطريقة مخصصة للاختبار الأغشية بمحاليل مختلفة تحتوي على عديد من الأملاح مثل : كلوريد الصوديوم والزيوت مثل الهيدروكربونات.

وقد أتضح من خلال هذه التحاليل والقياسات والتوصيفات بتحسن أداء الغشاء المعدل في عمليات الفصل والتنقية بشكل ملفت وكما كان متوقعاً نتيجة لتحسن خصائص الغشاء المخلتفة مثل : قابلية الغشاء للاتحاد مع الماء،و شحنة سطح الغشاء، وخشونته.

درجة الماجستير في العلوم

جامعة الملك فهد للبترول والمعادن

الظهران، المملكة العربية السعودية

أبريل 2021

CHAPTER 1

INTRODUCTION

1.1 Water and Desalination processes

The world population is growing rapidly and continuously, it is approximately 7.8 billion people according to 2020 world's population data sheet. Exceeding one billion of world's population have no access to cleaning water and around 70 % of world's population probably suffers from water shortage [1], [2]. Pure water availability on our planet cannot fulfill the needs of the whole world's population because the usable water percentage is considered very low compared to ocean water which is estimated to be around 97 % of total water resources on the planet as represented in figure 1.1 [3], [4]. Thus, there is a need for sustainable and cost-effective utilization of the largely untapped water source to solve this global crisis. The common solutions to substitute the current water shortage include water treatment and desalination. Desalination is a technique which tends to remove the salts from saline water to make it appropriate for human use and irrigation. It is considered a vital source for producing the pure water. As depicted in figure 1.2, the common two processes of water desalination are thermal and membrane processes. The most common thermal process is the distillation method which includes multi-stage flash (MSF), vapor compression (VC) and multiple-effect distillation (MED).

Whereas the common membrane processes are including electrodialysis (ED) and reverse osmosis (RO) [5], [6].

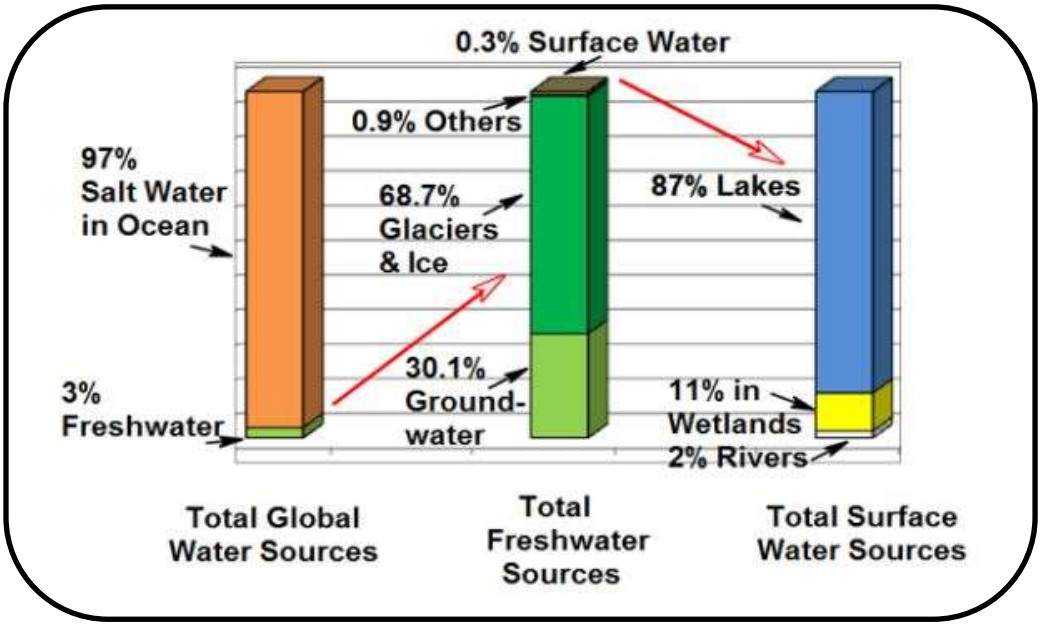

Figure 1.1 Water resources distribution on the planet [7].

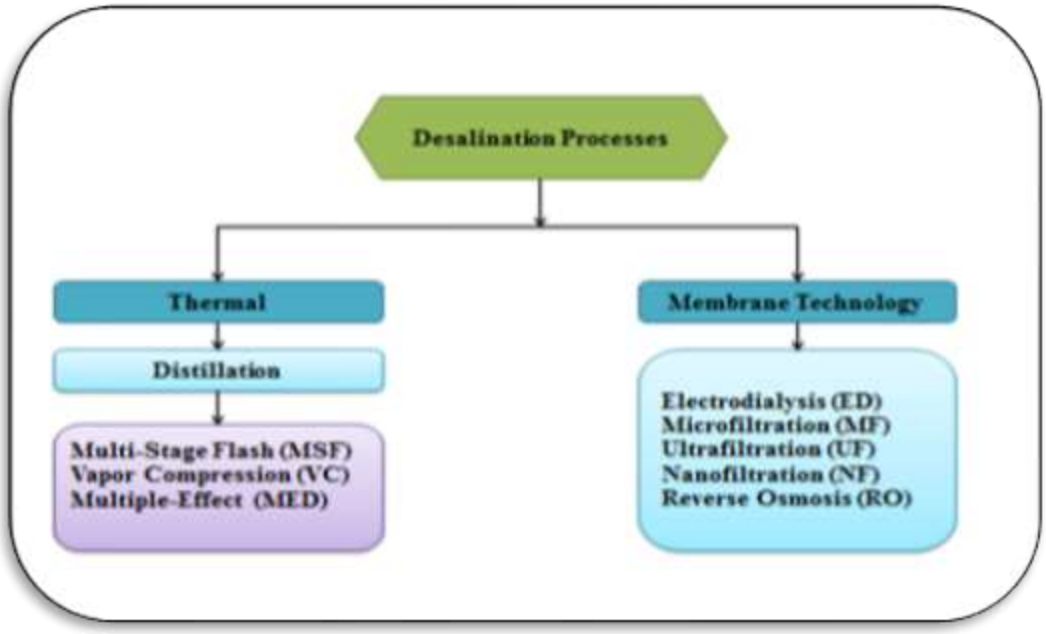

Figure 1.2 Water Desalination processes.

1.2 Membrane Technology

Membrane technology includes engineering methodologies for the transport of substances between two compartments with the use of semi-permeable membranes as shown in figure 1.3. In contrast to conventional thermal separation processes like distillation, membrane technology operates without heating, thus less energy is needed. Membranes are classified into different types including microfiltration, ultrafiltration, nanofiltration, reverse osmosis, forward osmosis, electrodialysis, and distillation membrane according to the used mechanism for rejection and pore size [7]. The reverse osmosis process (RO) is currently the most popular technique in membrane technology driven by pressure. It utilizes a semi-permeable membrane to remove fine contaminants of water with efficient separation performance and low energy requirements [8]. Improvements in the RO process mainly depend on the material used for the membranes so it becomes more applicable by developing thin-film composite (TFC) membranes. They have received great work since the polymerization process invention in 1965 by Morgan [9]. These types of membranes have the potential of overcoming the major drawbacks associated with this technique including low permeability and vulnerability to fouling. They are usually prepared by incorporating nanomaterials into polymeric materials using polymerization[10].

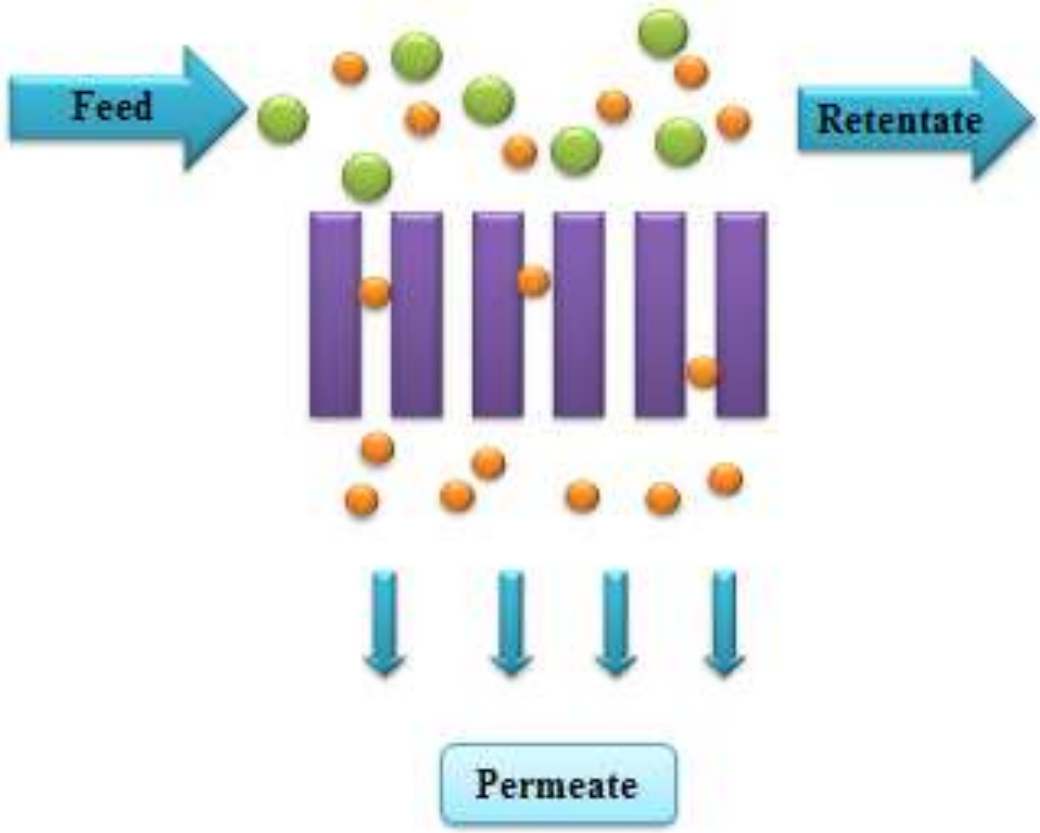

Figure 1.3 Schematic of membrane filtration process.

1.3 Reverse Osmosis (RO) Membranes

Polyamide TFC membrane is one class of nanocomposite membranes that have been largely used in RO due to its high performance in reducing energy usage in RO compared to other desalination processes including multi-stage flash and distillation thermal processes. Polyamide RO membranes typically consist of a porous polysulfone support layer at the middle, nonwoven fabric layer at the bottom that gives the membrane the mechanical strength to resist the high testing pressure, and a highly selective polyamide top layer (which controls the actual separation process) synthesized from

trimesoyl chloride (TMC) and m-phenylenediamine (MPD) [10]–[13]. Despite its favorable characteristics, PA membranes are still prone to fouling by microorganisms, colloids, and mineral scales [8]. The fouled membrane needs to be cleaned by harsh chemicals and ultimately replaced; both options are energy and cost consuming. As a result, most of the conducted research in the membrane area is focused on the reduction of fouling and improving polyamide membranes performance. Thus, many attempts were applied to adjust the surface of the membrane by chemical modifications including grafting several hydrophilic monomers onto the membrane, but the results are still not satisfactory [14].

One of the most innovative methods for mitigating the fouling, improving the permeate quality, and increasing the ion rejection of membranes is either by incorporating inorganic nanoparticles such as alumina(Al_2O_3), sliver (Ag), silica(SiO_2), and titania(TiO_2), or blending them into the porous membranes [13]–[15]. Using nanoparticles in membrane preparation gives a high degree to control the membrane fouling and provides a great ability to enhance the filtration performance of the membrane. Inorganic nanoparticles can also behave as adsorbents for different pollutants and noxious materials present in water including inorganic, organic, and bacterial pollutants, as well as toxic metal ions. This is because some inorganic nanoparticles like TiO_2 have catalytic properties, where combining the chemical oxidation with inorganic nanomaterial-based membranes can improve the resistance to membrane fouling and provide an enhancement in oxidative functionality. The strong oxidants O^{2-} and OH produced by these nanoparticles can lead to the decomposition and removal of different organic compounds on the membrane surface resulting in an enhanced membrane

performance [16], [17]. The incorporation of nanomaterials in polymeric membranes preparation has gained tremendous attention in the last decades because it is considered as a new methodology in enhancing the permeate flux and mitigating foulants deposition. Nanoparticles are incorporated into the membrane as fillers in the polymeric matrix of the membrane and there are common nanoparticles that are used including silica (SiO_2), TiO_2, and zeolites [16], [18].

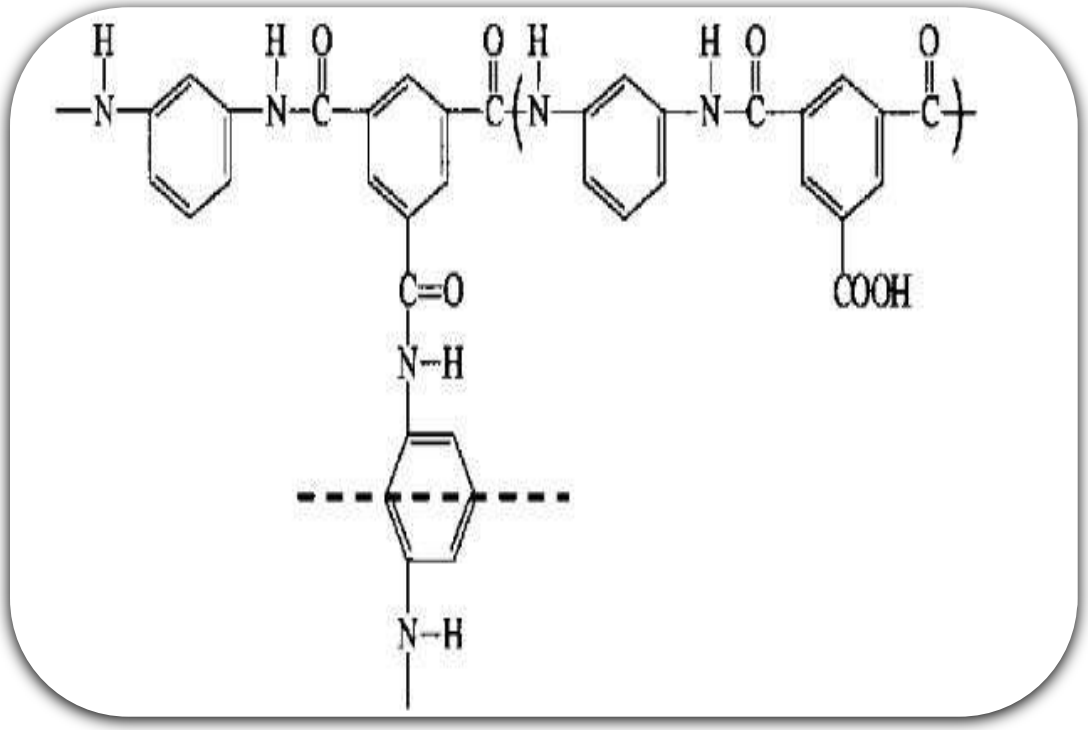

Figure 1.4 Molecular structure of polyamide.

CHAPTER 2

LITERATURE REVIE

2.1 The Preparation of the Thin-Film Composite (TFC) Membranes

Thin-film composite (TFC) membranes are highly selective and permeable membranes prepared mainly for water desalination. They are broadly used in nanofiltration (NF) and reverse osmosis (RO) processes. These membranes comprise many layers of different materials which are stacked together to produce one single membrane [19]. The main layers of TFC membranes are an ultrathin highly selective layer on the top, a much thicker porous support layer at the middle, and nonwoven fabric layer at the bottom that gives the membrane the mechanical strength to resist the high testing pressure. The active top layer of the TFC membranes is around 200 nm thick and is made from polyamide. For the intermediate layer, its thickness is about 50 μm and it is prepared by phase inversion processes. Different polymers such as polysulfone(PSF), polyethersulfone (PES), polyphenylene oxides, polycarbonate, poly(styrene-co-acrylonitrite), polyacrylonitrile, poly(phthalazinone ether sulfone ketone) (PPESK), polypropylene, polyetherimide, and others are used to synthesis the intermediate support[20]–[23]. However, polysulfone (PSF) and polyethersulfone (PES) are chosen to be the best materials for the support layer of membranes because they were tested to have high resistance against compaction, reasonable stability in an acidic environment, and

preferable flux. Moreover, nonwoven fabric layer at the bottom is about 120 μm and is mostly made of polyester [24], [25]. The active top layer is fabricated using aromatic polyamide (PA) and considered as the basis of the TFC membranes because it is the layer that will determine the permeability and selectivity of the membrane so most of the researches has been focused on enhancing its properties [26]. The most utilized process of manufacturing the membrane active layer is in situ polymerization (IP) of 1, 2-phenylenediamine (MPD) and trimesoylchloride (TMC). During the preparation of the active layer, it is significant to optimize the pore size of the produced membranes by controlling the polymerization reaction variables in such a way that achieves a higher salt rejection. In addition, its thickness should be reduced to ease the permeate transfer [25], [27], [28].

2.2 Thin-Film Composite Membranes Modifications Using Inorganic Nanoparticles

The continuous enhancement of thin-film composite membranes has resulted in making the membranes more permeable by a factor of 1.5-2 than before, but they are still degradable in the presence of chlorine, making cleaning complicated and leading to fouling [25]. The most common problem in the polymeric membrane is the easiness of fouling. This critical limitation is due to the precipitation and deposition of chemicals, colloids, and microbes on the surface or pores of the membrane, so it requires significant attention because it can lead to high energy consumption, costly cleaning, and membranes replacement [29]. In order to reduce membrane fouling and improve

membrane performance operation, membrane surfaces can be treated by any chemical method such as grafting few hydrophilic monomers on membranes but the reduction of fouling is not satisfactory. Furthermore, the recent developments of nanotechnology (using nanoparticles) have emerged to the synthesis of the membrane to enhance the synergistic effects of membrane on water treatment. Nanoparticles-based membranes can have beneficial effects on fouling reduction [29]–[32].

Various inorganic nanoparticles of 2-100 nm size are used as fillers in the polymeric matrix including silica(SiO_2), zeolites, titania(TiO_2), sliver(Ag), alumina(Al_2O_3), graphene oxide(GO). These nanoparticles are added to the polymeric membranes to promote membrane operation performance (enhancement of permeate quality and flux), to give a high ability to control the fouling resistance and to form the desired structure [14]. The inorganic nanoparticles such as TiO_2, Al_2O_3, and SiO_2 have been combined into polymeric membranes for mitigating different types of fouling including inorganic fouling, organic fouling, and bacterial growth affecting the polyamide membranes [14]. They can also provide a superb change on the contact angle measurement; the contact angle can be minimized by increasing the concentration of nanoparticles. For example, the contact angle of poly(vinylidene fluoride) (PVDF) membrane at 0 % Al_2O_3 is 84^o, but increasing Al_2O_3 concentration to 2-4 % leads to a decrease in the contact angle to 57^o-59^o [33]. Titania (TiO_2) has been considered as promising nanomaterials for water desalination [30], [31]. Titania nanoparticles incorporation in water purification can oxidize or reduce the organic and inorganic toxic compounds in water. These nanoparticles have been utilized to degrade organic compounds including dioxins, chlorinated alkanes, and benzenes, and minimize toxic metal ions. Thus, these inorganic

nanoparticles are used for the purpose of improving membrane performance variables including permeability, strength; selectivity, fouling resistance. In addition, they can be used for water disinfection. The main objective of embedding titania into the aromatic polyamide membrane is to reduce biofilm formation. Titania addition to polyamide membrane will give membrane higher photocatalytic bacterial efficiency. These nanoparticles have the capability to kill microbes and reduce the different foulants without producing any harmful materials [13]. The photocatalysis of TiO_2 is occurring under light by oxidation or reduction reaction to produce different active oxygen species including hydrogen peroxeid which are able to kill microbes and decompose organic compounds [25], [34], [35]. Titania is assembled to membrane surface through ionic bonding and hydrogen bonding with carboxyl functional groups (-COOH) of polyamide [36].

Other common inorganic nanomaterials used for enhancing the membrane operations include graphene, graphene oxide, and carbon nanotubes. Graphene is defined as a sheet consisting of carbon atoms that are strongly packed to form a hexagonal matrix. Graphene has astonishing characteristics compared to polyamide layers. It has a thickness of about 1∼2 nm and it is considered as stronger as and more chemically active than polyamide so it is largely used in membrane production in the last years. Graphene oxide is in the form of two-dimensional(2D) nanosheets that are used to make the membrane more novel by simple layer-stacking methods, providing high flexibility to adjust the interlayer spacing, functionality, and charge of the GO-based membrane to enhance filtration and separation efficiency [37]. The thickness of graphene oxide can be controlled easily by changing the number of graphene oxide sheets. GO has various

remarkable properties such as high antibacterial, and photocatalytic that give GO huge potential to enhance the removal of contaminants and fouling reduction [38]. GO is also used specifically for Forward Osmosis by the assembly of layer-by-layer of graphene oxide to produce better stability membrane (interlayer crosslinking) and using polyelectrolyte on both sides of the support layer [37]. The produced membrane has more reduction of concentration polarization due to the separation of both sides of its support layer [25]. GO was combined with aromatic polyamide in membrane synthesis by incorporating it into the polymeric matrix of support or active layer polyamide membrane. By this process, nanofiltration membranes of high positive charge are improved. The enhanced membranes have attained a high salt rejection of $Na^{+}$and Mg^{2+} ions with 38.1 % and 93.9% respectively and a high water flux [39]. Swelling is a common problem of GO membranes due to the interlayer spacing enlargement. It causes the ionic solute flux to be higher. This issue can be fixed by adjusting the building blocks of GO (nanosheets of GO) properly (by chemically cross-linked). As swelling is mitigated, solute flux is decreased [37]. GO can also be incorporated into the support layer of polysulfone (PSF) by phase inversion process and it enables to produce of more water flux than a pristine PSF support layer by a factor of three times [40]. The optimum addition of GO to a PSF membrane to achieve a favorable PSE/GO support layer in terms of pore size, porosity, and thickness has been estimated to be (0.25 wt %). Exceeding a certain value of GO addition approximately (≥ 0.5 wt %), there will be a decline for performance parameters of the membrane such as permeation, and selectivity due to the significant change in structure and GO dispersion [40]. Carbon nanotubes and metal oxide nano-particles used in membrane manufacturing can increase

the resistance against fouling, make membrane materials more novel, and enhance the permeability and permeate quality of water. Polymeric membranes made of carbon nanotubes or fullerenes have more permeability than the bare ones [38]. Carbon nanotubes based membranes can be considered as the basic type of membranes to reduce the fouling by inhibition the growth of bacteria. Carbon nanotubes (CNTs) can also be added to PVDF [41], whereas Multi-walled carbon nanotubes (MWCNT) can be injected into PSF [42]. In general, for producing excellent –performance membranes (high selectivity and water flux), it is extremely significant to modify the structure of the support layer of the membrane to minimize the résistance to the transport of solutes [43]. Observations of using nanoparticles in membrane manufacturing can be summarized in improving the functionality and durability of the membrane by increasing layer thickness, increasing the porosity of skin surface, and increasing the permeability of the membrane (sometimes it is observed a decrease in the permeability of membrane). However, the reduction of different fouling types including organic, inorganic, bacterial fouling is one of the main goals of using nanoparticles in membrane production. Fouling mitigation is mostly combined with the improvement of flux while using the nanoparticles but porosity improvement is relatively independent of the concentration of used nanoparticles [44].

2.3 Graphene Oxide

Graphene oxide nanosheets with a thickness of approximately 1.1 ± 0.2 nm are characterized by their high rate of water transport due to the interlayer spacing of GO nanosheets that may serve as water channels, therefore they have been incorporated into the polymeric membranes to enhance the overall efficiency of the membrane [45]–[49].

Functional groups present in GO such as epoxy, hydroxyl, and carboxyl groups have a significant ability to disperse in different polar solutions compared to other nanomaterials. This feature of GO makes the nanosheets and polymers more compatible with each other [49]. GO is so hydrophilic because the polar functional groups present on GO surface form hydrogen bonds with water molecules [50]. GO with higher hydroxyl functional groups is more stable than GO with a high content of epoxide groups [51], [52]. Graphene oxide-based membranes are more permeable to polar solvents compared to other membranes types due to graphene oxide swelling, this swelling state also makes the membrane more permeable to the undesired solutes [53]. GO also has a tremendous ability to strengthen the mechanical properties and stability of the membranes to withstand high pressures [49]. Water flows smoothly through GO layers without any friction due to the hydrophilicity and smoothness of graphene atoms. Besides, the embedding of GO into the polyamide membrane can significantly improve the anti-fouling property and flux of the membrane as well as it can effectively enhance membrane hydrophilicity [54].

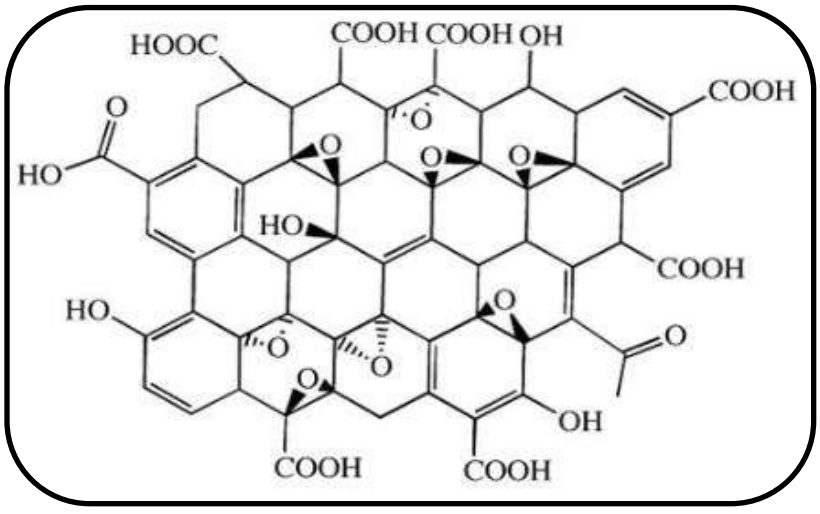

Figure 2.1 Molecular structure of Graphene Oxide [17].

2.4 Titania (TiO2)

Anatase TiO_2 (the most stable type of titania compounds) is the cheapest and the most available photocatalyst. It is known as a hydrophilic nanomaterial and has a significant antibacterial fouling potential [13], [55]. It also has high reactivity and chemical stability. In addition; it is a nontoxic material, environmentally friendly, and easy to synthesize [56]. Furthermore, TiO_2 particles have a poor adsorbing affinity toward organic molecules especially the hydrophobic organic molecules [13], [56]. TiO_2 particles are strongly adhered to the membrane surface by bidentate coordination and a hydrogen bond [13]. As a result, it is usually embedded in the thin film polyamide membrane to enhance permeability and biofouling resistance. TiO_2 is loaded on other nanomaterials to improve its photocatalytic performance and wastewater treatment effect [56], [57].

Table 2.1 Literature review summery

Authors	Findings	Limitations
(Lee et al., 2008)	- Polyamide (PA) nanocomposite membrane was modified by high loading of TiO_2 nanoparticles. - It showed high and stable rejection value of more than 95% with respect to $MgSO_4$ and the flux of 9.1 L/m^2h.	1. Permeability was low. 2. Hydrocarbons rejection was not studied. 3. Monovalent ions rejection was not tested.

(Lind et al., 2009)	- Zeolite-polyamide thin film nanocomposite membrane was formed onto the polysulfone layer. - Permeability, NaCl, $MgSO_4$ and poly (ethylene glycol) rejections were tested under 1550 kPa. - Permeability was increased and rejection was remained similar to the bare membrane.	1. Salt rejection was not improved. 2. Less number of organic samples has been studied.
(Xu et al., 2011)	- The surface of the polyamide membrane was treated by chlorine, followed by supramolecular assembly of chitosan. - Led to a charge reversal due to skin layer of chitosanium. - It exhibited a permeation flux of 57.7 L/ m^2 h and a salt rejection of 95.4% with respect to 1500 ppm NaCl and at 0.8 MPa.	1. Organic pollutants were not studied. 2. Polyamide membrane is sensitive to chlorine attack and can be degraded using chlorine in coating. 3. Higher pressure will lead to increase the temperature of the tank.

(Saleh & Gupta, 2012)	- Polyamide membrane was modified using alumina nano-particles. - The permeate flux was improved due to the enhanced hydrophilicity - The salt rejection (1000 ppm NaCl, 1000 kPa) was maintained constant.	1. The impact of alumina nanoparticles on solute rejection was not significant. 2. No divalent ions or hydrocarbons studies.
(Rajaeian et al., 2013)	- The polyamide membrane was modified using TiO_2. It was tested at 760 kPa and 2000 ppm NaCl. - Water flux was increased up to 2-fold.	1. Salt rejection remained the same. 2. Tested only the monovalent ions (Cl^-). 3. Not studied the hydrocarbons rejection.
(Zhao et al., 2014)	- The polyamide membrane was improved by incorporation of modified multi-walled carbon nanotubes. - Flux of polyamide/MWNT membrane increased 14.86 to	1. Salt rejection decreased slightly.

	28.05 L m^{-2} h^{-1}. - (NaCl, 2000 ppm) was studied at 1600 kPa. - It showed better antifouling and antioxidant properties.	
(Peyki, Rahimpour, & Jahanshahi, 2015)	- Thin film composite membrane was modified using SiO_2 nanoparticles to test permeability and NaCl rejection. - Hydrophilicity and flux were increased.	1. Slight decline in rejection. 2. Very high pressure around 4400 kPa. 3. Hydrocarbons and divalent ions rejection were not tested.
(Yin et al., 2016)	- A PA membrane was synthesized by adding graphene oxide nanosheets. - The permeate flux under 300 psi increased from 39.0 ± 1.6 to 59.4 ± 0.4 L/m^2 h. - The membrane showed excellent stability.	1. NaCl and Na_2SO_4 rejections slightly decreased respectively. 2. Study was under high pressure.
(Li, Li, & Zhang,	- Carbon dots (CDs) were successfully incorporated into	1. Not focused on divalent ions and organic

2017	the polyamide layer of the membrane. - The membranes with 0.02 wt% CDs loading exhibited high flux and improved NaCl rejection at 1550 kPa.	pollutants rejections.
(Al Mayyahi, 2018)	- TiO_2 nanoparticles were inserted into the polyamide layer of traditional thin film composite membrane. - TiO_2 could effectively improve the NaCl rejection and permeability.	1. High pressure at around 2070 kPa.
(Ahmad, Goh, Wong, Zulhairun, & Ismail, 2020)	- The membrane was fabricated by embedding titania nanosheets (nTNS) on the surface of polyamide (PA). - The NaCl rejection and permeability were improved and achieved the highest values with 2 bilayers of TNS at 1600 kPa	1. No divalent ions rejection study.

	and 2000 ppm NaCl.	

To sum up, the developments of a polymeric membrane with high permeate flux and ion rejection continues to remain the main challenge for researchers to overcome. Modification of polymeric membrane by inorganic nanomaterials is one of the most innovative methodologies to mitigate the fouling, improve the permeate flux, and increase the ion rejection. As explained previously, several studies have been conducted on the incorporation of inorganic nanoparticles into polymeric membranes including alumina (Al_2O_3), graphene oxide (GO), and titania (TiO_2), silica (SiO_2), and zeolites. However, the research room is still promising for further improvements including the use of combination of inorganic nanomaterials. Titania is known as a hydrophilic nanomaterial and has a significant antibacterial fouling potential. It is usually embedded into the thin film polyamide membrane to enhance the permeability and biofouling resistance. Furthermore, it showed high and stable rejection value of the inorganic salts. Graphene oxide (GO) nanosheets are characterized by their high rate of water transport due to the interlayer spacing of GO nanosheets that may serve as water channels. Water can flow smoothly through GO layers without any friction due to the hydrophilicity and smoothness of graphene. GO also has a tremendous ability to strengthen the mechanical properties and stability of the membranes to withstand high pressures. Graphene oxide added into the membrane showed excellent stability and enhancement of the permeability. As a results, titania chemically bonded to graphene oxide (TiO_2-GO) was selected to be incorporated into the membrane for further improvements in the membrane

performance. GO was used as a nanoscale substrate to form TiO_2 to produce a hybrid that contains enhanced properties of both GO and TiO_2. TiO_2-GO compound was added into the aqueous MPD solution and TMC in organic solution and incorporated into the polymeric matrix. To study the effect of TiO_2-GO compound on the performance of the PA membrane, the performance parameters of the membrane including permeate flux, salt rejection, and oil rejection were evaluated using a custom-made laboratory setup.

2.5 Objectives

This research work aims to formulate nanomaterials that can be incorporated into polyamide membranes for application in water purification.

The specific objectives are:

- To prepare the materials including MPD, TMC, and TiO_2-GO compound as a material for the thin-film polyamide membrane.
- To prepare the polyamide membrane using polymerization of the different prepared materials.
- To evaluate the performance of the modified membrane in terms of permeate flux and ion rejection.

CHAPTER 3

EXPRIMENTAL

3.1 Materials

Graphite powder , Titanium dioxide(TiO_2), nitric acid(HNO_3), sodium nitrate($NaNO_3$), sulphuric acid(H_2SO_4)(98%), potassium permanganate($KMnO_4$), titanium tetraisopropoxide($C_{12}H_{28}O_4Ti$), m-phenylenediamine(MPD), sodium chloride, sodium sulfate(Na_2SO_4), tridecane($C_{13}H_{28}$), isoocatane(C_8H_{18}), dodecane($C_{12}H_{26}$), toluene(C_7H_8) , industrial-grade n-hexane (a mixture of isomers), and trimesoyl chloride(TMC) were obtained from Sigma Aldrich and were utilized as received. Microporous polysulfone support layer was brought from Sterlitech. The used water for whole experiments and solutions was distilled water. All materials and chemicals used in the whole process were with high purity so they were used directly without any further purification.

3.2 Synthesis of Titania-Graphene Oxide (TiO_2-GO) Compound

Graphene oxide was derived using graphite following Hummer's method. Graphite powder (2 g) and $NaNO_3$ (2 g) were added to 90ml of H_2SO_4 (98%) in an ice medium (0-5ºC) under stirring. After 4hrs of stirring the mixture, $KMnO_4$ (12 g) was slowly introduced into the mixture with care keeping the temperature below 15ºC. Afterward,

184 ml of water (H_2O) was slowly introduced to dilute the system and stirred continuously for 2 hrs. The components were then kept under stirring at 35-40 °C for 2 hrs after removing the ice bath. Then, it was refluxed at 100 °C for about 15 min. Then, the temperature was adjusted at 30°C and the system was kept until the brown color is observed, and under the addition of H_2O_2, bright yellow was observed. 0.2 L of water was introduced under stirring. After 1h, the stirring was off and then the filtration was performed using a centrifuge with also washing using 1M HCl and then followed by DI water till pH was neutral. The collected GO was dried under a vacuum. Graphene/titania was synthesized by dispersing GO in 5% alcohol aqueous media by a sonicator. 3% titanium tetraisopropoxide was added under stirring. The components were kept under reflux for around 6 h at 100 °C. Then, the heating was switched off. The obtained product was separated, dried. Then, it was calcinated at 623°C for 3hrs.

3.3 TiO_2-GO Membrane Preparation

A piece of a microporous polysulfone support layer with approximately 100 μm thick, was cut and immersed in activation solution that was diluted with distilled water for 1 day to fully activate the whole surface of the support and wet all its pores, and then it was dried for 2 h. The polysulfone support was then submerged in a solution composed of 0.005 g/ml MPD and 0.001 g/ml TiO_2-GO at an ambient temperature for 2 min in a way that allows only for the top part of the PSf support to absorb the solution. After removing it from the solution, it was moved by a special tool in different directions to distribute the solution on the surface evenly and to take off the excess of the solution. After that, it was dried for 30 min under vacuum and then immersed in a solution of

0.0025 g/ml of TMC for 5 min. After 5 min, the membrane was removed from TMC solution and moved by a specific tool for 5 min to diffuse the solution equally on the whole surface and remove the excess amount of TMC solution. Finally, it was dried under vacuum and kept in a glass plate for activation until use. The previous procedures were used to prepare different membranes with one, four, and eight layers.

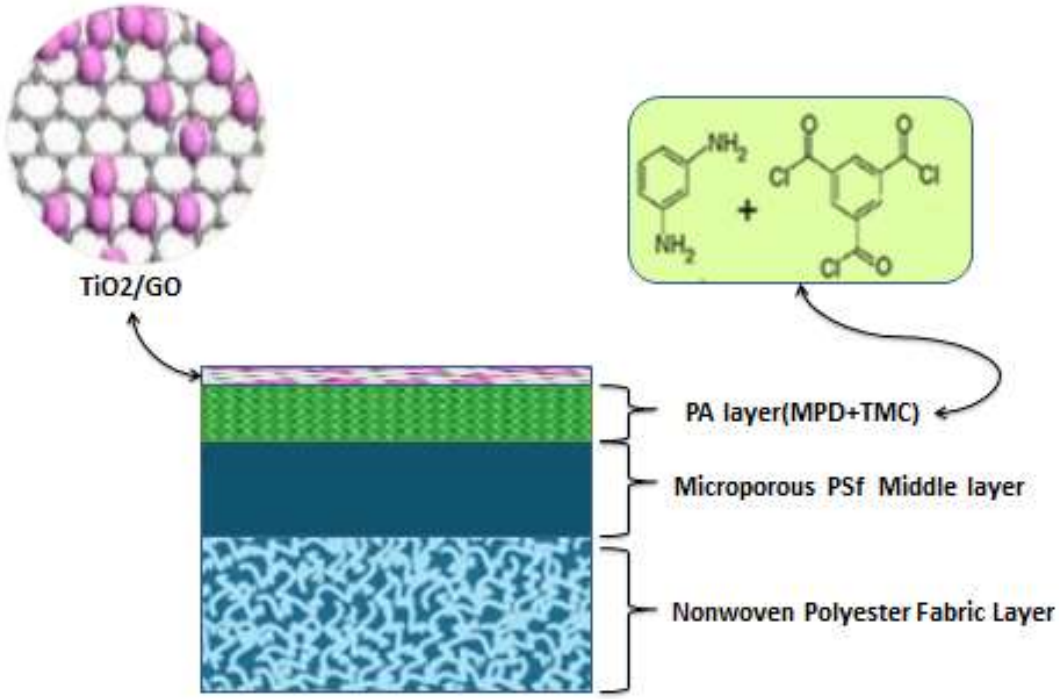

Figure 3.1 Polyamide membrane shows layers and the embedded nanoparticles.

3.4 Characterization Methods

Different characterization methods were utilized to analyze TiO_2-GO compound and modified membranes. Fourier Transform Infra-Red (FTIR) spectroscopy (Smart iTR NICOLET iS10) and X-ray photoelectron spectroscopy (XPS) (ESCALAB 250Xi) were applied to characterize the chemistry of the prepared materials. In addition, X-ray diffractometer (XRD) (D-5005D-5005) was applied to characterize the crystalline phases and average crystalline size of the as-synthesized TiO_2-GO compound. To analyze the effects of surface modification on the membrane morphology, a field-emission scanning electron microscope (FESEM, Tescan Lyra-3, Dual Beam, Tescan), equipped with an energy dispersive x-ray spectrometer (EDX, Oxford Instruments) was performed. Before applying the analysis, the different specimens were coated with a thin layer of gold using a sputtering process to make them electrically conductive. Atomic force microscope analysis was utilized to study the surface morphology and surface roughness parameters (average surface roughness (R_a), a difference in height between the top and valley (R_{max}), and root mean square (RMS) of the polyamide membrane using Agilent 5100 SPM instrument equipped with a controller Picoscan (Agilent Technologies, Tempe AZ, USA) coupled with a standard SiN cantilever) and estimate the surface roughness variables values. Membrane samples of area 1 cm^2 were put on a glass plate by tape and the measurements were taken at different locations to reduce the experimental error and obtain better accuracy. To analyze the hydrophilicity and wettability of the membrane, a contact angle was calculated using an Attension Theta Optical Tensiometer (Biolin Scientific, Finland). The measurements were taken at 5-6 random locations and averaged to reduce the experimental errors. To study the surface chemistry of membranes and

determine the functional groups present in TiO_2-GO compound, Fourier Transform Infra-Red (FTIR) spectroscopy (Smart iTR NICOLET iS10) in 400-4000 cm^{-1} wavelength range was applied. Before performing the membrane characterization, background correction was performed by scanning the empty stage. Finally, the collected spectra were identified by the intensity of functional groups. To characterize TiO_2-GO compound, pellets of TiO_2-GO were prepared by blending samples of TiO_2-GO with KBr and pressing them at room temperature. X-ray photoelectron spectroscopy measurement (XPS) (ESCALAB 250Xi) under ultra-high vacuum conditions and on an Axis Ultra DLD was performed to confirm nanoparticle presence on the membranes by studying the surface state and the different bonds in the samples. 1 cm^2 of the coated membrane before and after testing, TiO_2-GO compound pellet was prepared. Then the analyses were conducted. The binding energy range of N 1s, O 1s, C 1s, and Ti 2p, and survey scans was 0-1000 eV with a 1 eV resolution.

3.5 Modified Membrane Performance

Filtration parameters of the membrane were tested after each surface treatment. The modified membranes were tested at ambient temperature and a pressure of 1 MPa (10 bars) through the filtration system provided by Sterlitech. The membrane filtration system has a membrane cell with an area of 35 cm^2 connected to the feed tank and the pump by Teflon and stainless steel tubes as represented in figure 3.2. Membranes with different layers were first compacted in 5 L of distilled water for 3 h at 1 MPa (10 bars) before taking the measurements of water flux. Salt rejection of membrane was studied by

adding 2000 ppm concentration of salt (NaCl) and 1500 ppm of Na_2SO_4 salt respectively to the feed tank. NaCl and Na_2SO_4 salts have the highest concentration in the seawater. Therefore they are considered as models for testing the performance of the modified membranes [58]. Considering seawater contaminated with oil, the hydrocarbons rejection was tested using solution models which were prepared by mixing saltwater and oils. The saltwater was prepared with 2000 ppm NaCl. Then, this solution was spiked with toluene, dodecane, isooctane, and tridecane, 500 ppm of each (total 2000 ppm). Finally, the breakthrough of the membrane was investigated by studying the effect of feed concentration on salt rejection at different high concentrations of NaCl solution. The effect of layers coating on the salt rejection was analyzed. The experiment was conducted and the concentration of salt was measured by Ion Chromatography while oil was monitored by GC-head space. The system was running for 2 h to equilibrate before measuring the permeate water flux and salt rejection. The solution was stirred constantly to avoid any concentration polarization effect. Then, the permeate flux was collected in a graduated cylinder at a specific interval of time, whereas the concentrate was returned to the feed tank to keep the salinity of water constant. The collected samples of permeate and feed waters were tested by Ion Chromatography chemical analysis (930 Compact IC Flex). Experiments were taken two times for each sample and then averaged. Salt rejection(R) and permeate water flux (J) are calculated using these two equations.

$$R = \left(1 - \frac{C_P}{C_F}\right) \times 100 \quad , \quad J = \frac{V}{At}$$

The parameters in the previous equations are conductivity of feed water (C_F), permeate water conductivity (C_P), permeate time (t), and permeate volume (V), and membrane area (A).

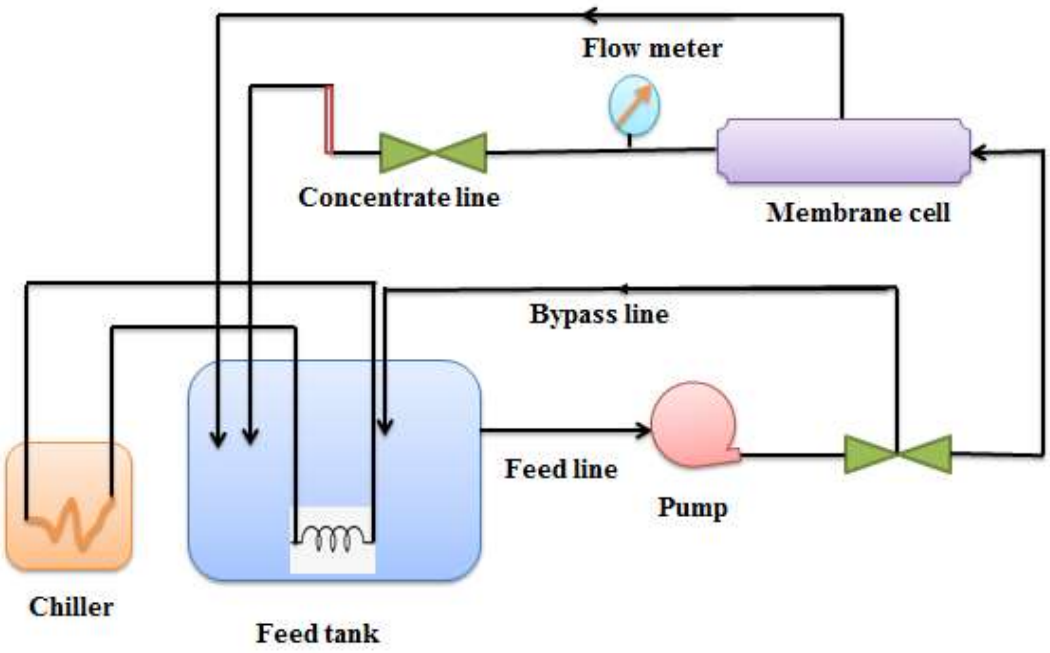

Figure 3.2 Schematic sketch of the lab-scale setup for membrane filtration.

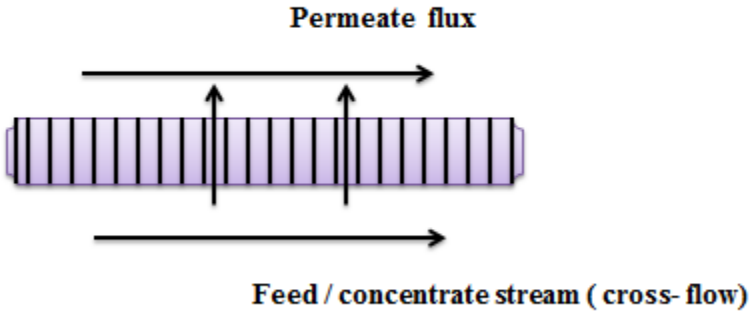

Figure 3.3 Cross-flow membrane cell of the filtration system.

CHAPTER 4

RESULTS AND DISCUSSION

4.1 TiO_2-GO Compound Characterization

4.1.1 X-Ray Diffraction

The X-ray diffractometer (XRD) is performed to identify the crystal structure of as-synthesized TiO_2-GO compound. The X-ray diffraction patterns of GO, TiO_2 and TiO_2-GO compound are depicted in figure 4.1, 4.2 and 4.3 respectively. As can be observed in figure 4.1, the XRD of GO shows a sharp peak at $2\theta \cong 11°$ which is assigned to (001), and another peak at $2\theta \cong 43°$ that is attributed to (100) [59]. The XRD patterns of titania depicted in figure 4.2 represent the sharpest peak at $2\theta \cong 25.5°$ that is ascribed to (1010) and the other peaks shown at $2\theta \cong 37°, 48°, 54^{\circ}, 55^{\circ}, 62^{\circ}, 69^{\circ}$ and $75°$ that indicate to (004), (200), (105), (211), (204), (116), (220), and (215) respectively [60]. These different peaks can prove that the present titania is in the anatase phase and has a tetragonal structure. Furthermore, the XRD patterns of TiO_2-GO compound exhibit a weak at $2\theta \cong 24.5$ which indicates to the graphene sheets in the compound material and the sharpest peak shown at $2\theta \cong 25.6°$ is assigned to (110) of the anatase phase of TiO_2 nanoparticles [41], [61]–[63]. The other reflection peaks of the compound are also similar to those shown by the XRD of pure titania so they can prove the presence of the anatase phase of TiO_2 nanoparticles.

The sharp XRD peaks in figure 4.3 indicate the excellent crystalline structure of TiO_2 nanoparticles. The obtained results are strongly consistent with other authors [64]–[66]. XRD patterns confirm that the TiO_2 particles in our compound are entirely anatase phase which assures the highest photoreactivity and best efficiency in annihilating the microorganism. As can be observed, GO peaks have overlapped with the peaks of titania and not appeared on the compound. This is due to the dispersion of the titania on graphene. These results indicate that titania was successfully dispersed on graphene nanosheets [65], [67], [68].

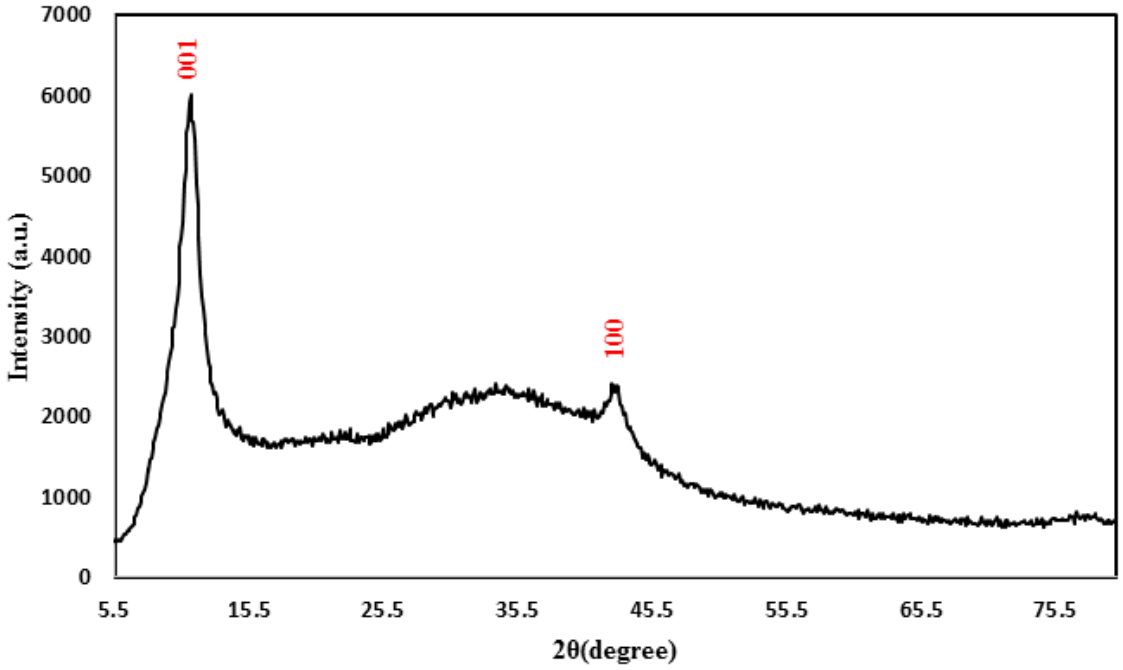

Figure 4.1 The XRD patterns of graphene oxide (GO).

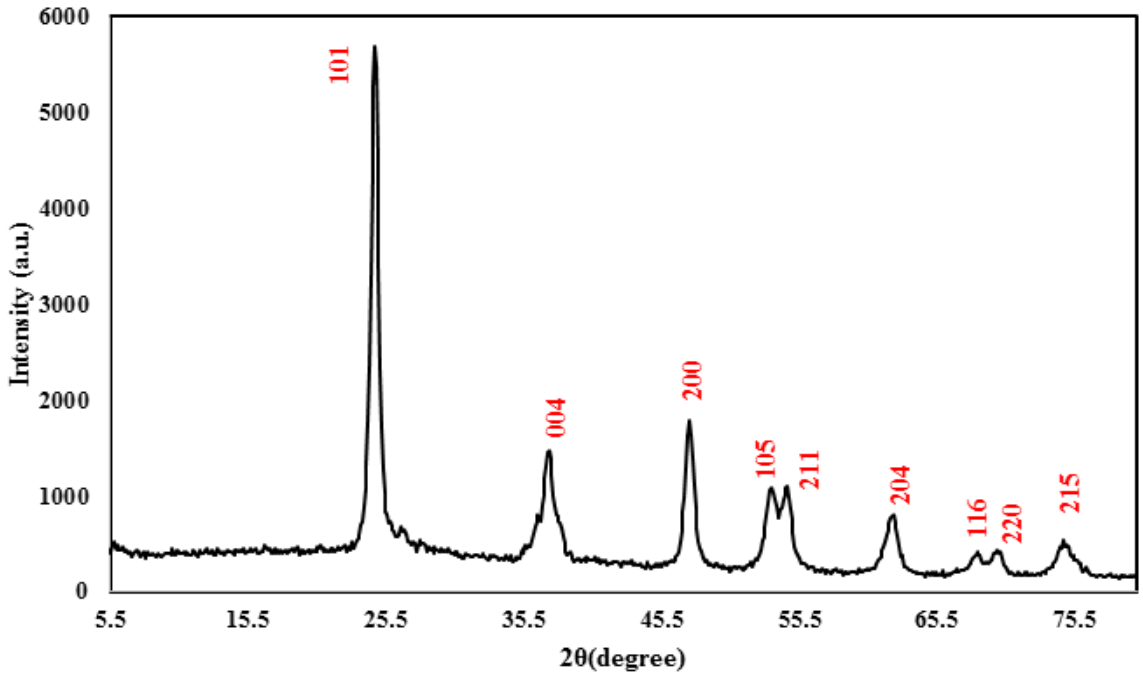

Figure 4.2 The XRD patterns of titania (TiO_2).

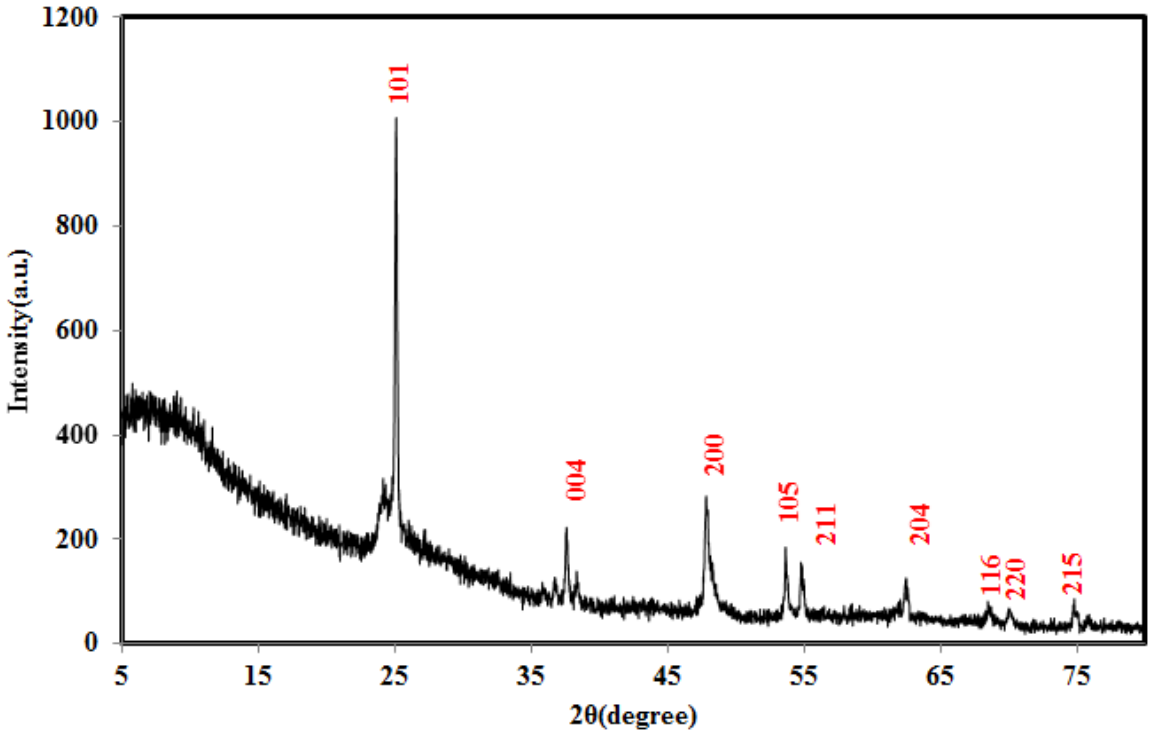

Figure 4.3 The XRD patterns of TiO_2-GO compound showing all the characteristic peaks.

4.1.2 X-Ray Photoelectron Spectroscopy (XPS)

X-ray Photoelectron Spectroscopy (XPS) was utilized to analyze the surface chemistry of TiO_2-GO compound. XPS results of TiO_2-GO compound are represented in figures 4.4 - 4.7. As can be observed, The titanium(Ti 2p) spectra depict two peaks, the first peak is at binding energy around 458.70 that is related to Ti $2p_{3/2,}$ and another peak at around 464.50 eV attributed to Ti $2p_{1/2}$ [68]. It can be noted that Ti $2p_{1/2}$ is much broader than Ti $2p_{3/2.}$ The peak values of Ti 2p are in agreement with the Ti^{+4} value in the TiO_2 lattice. The peaks of Ti 2p are consistent with those reported by other authors [69], [70]. The spectra of O 1s have the characteristic peak at around 529.2 eV which is attributed to the Ti-O bond and it is in harmony with the binding energy of the oxygen ion (O^{-2}) in the lattice of titania. Furthermore, the shoulder peak sets at about 531.0 eV were assigned to adsorbed OH^- on the titanium dioxide surface [68]. For the spectra of the carbon (C 1s), the major peak was shown at about 284.7 eV, which is associated with C-C and C=C bonds. Another peak was observed at around 287.5 eV, which indicates to the C=O bonds [71]. When GO reacts with TiO_2, a significant no. of oxygen-containing groups are consumed in the nucleation and growth of TiO_2 crystallites, and so the GO is reduced [68]. As a result, when GO reacts with TiO_2, bonds between them are formed. Other bonds present in GO expected to appear are C-O-H and O=C-OH and they were neglected due to the weak signal [66].

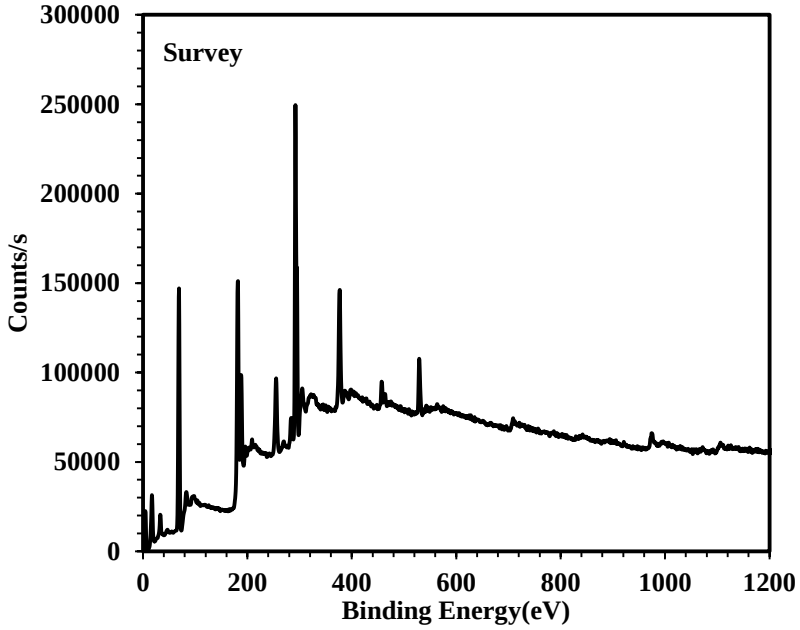

Figure 4.4 High resolution XPS survey spectra of TiO_2-GO compound.

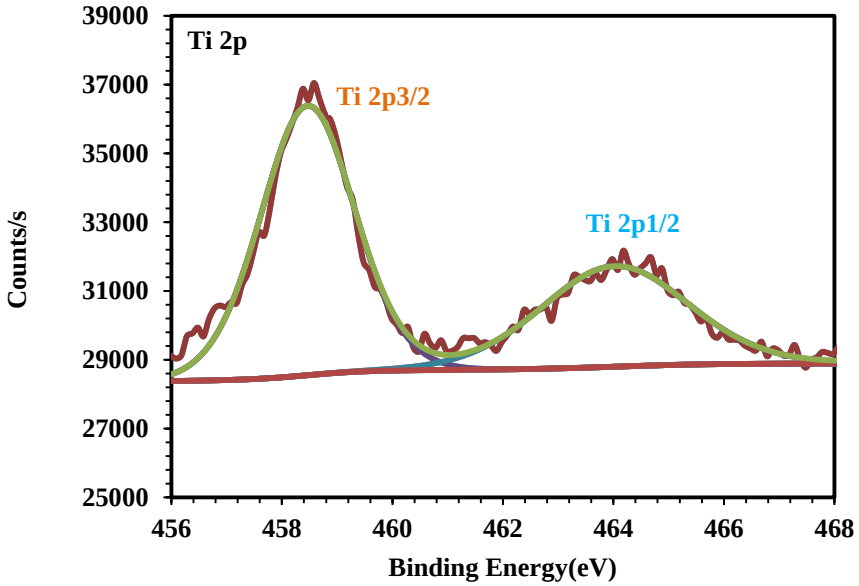

Figure 4.5 High resolution XPS Ti 2p spectra of TiO_2-GO compound.

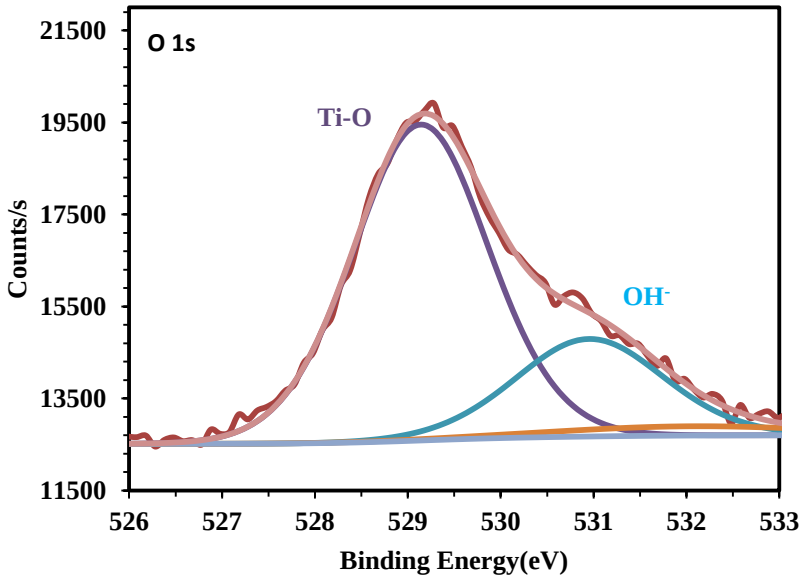

Figure 4.6 High resolution XPS O 1s spectra of TiO_2-GO compound.

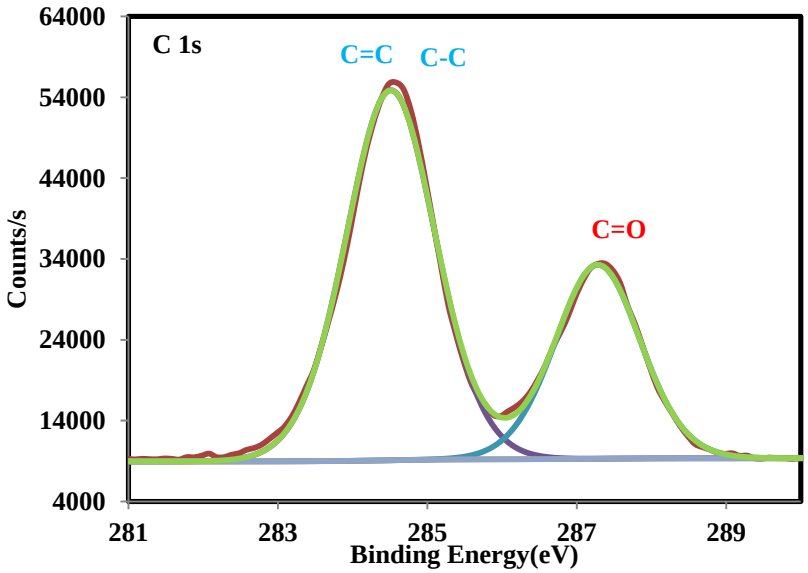

Figure 4.7 High resolution XPS C 1s spectra of TiO_2-GO compound.

4.1.3 Fourier Transform Infra-Red (FTIR)

Fourier Transform Infra-Red (FTIR) spectroscopy was performed to identify the major functional groups found in the TiO_2-GO compound. Characteristic FTIR spectra of TiO_2-GO compound are demonstrated in figure 4.8. As can be seen, FTIR of TiO_2-GO shows a broad absorption peak at around 3384.2 cm^{-1} indicated to the O-H stretching vibrations of adsorbed H_2O and Ti–OH group. This specific group gives the compound the ability to be dispersive in water and make it more hydrophilic material [66], [70], [72], [73]. The peak at around 1627.6 cm^{-1} is associated with the stretching vibration of carbonyl(C=O) and C=C groups[66], [74], [75]. The weak band that appeared at around 1276 cm^{-1} can be related to Ti-O or C-O-C bonds. Another weak peak shown at about 1068 cm^{-1} can indicate C-O bonds [66], [76]. These surface oxygen-containing functional groups provide the possibility of covalent bonding of TiO_2 onto the GO surface. The broad peak absorptions shown at low frequencies lower 1000 cm^{-1} are related to the vibration of Ti-O-Ti and Ti-O-C [73], [77]–[79]. This indicates that TiO_2 particles were strong chemically bonded to the GO.

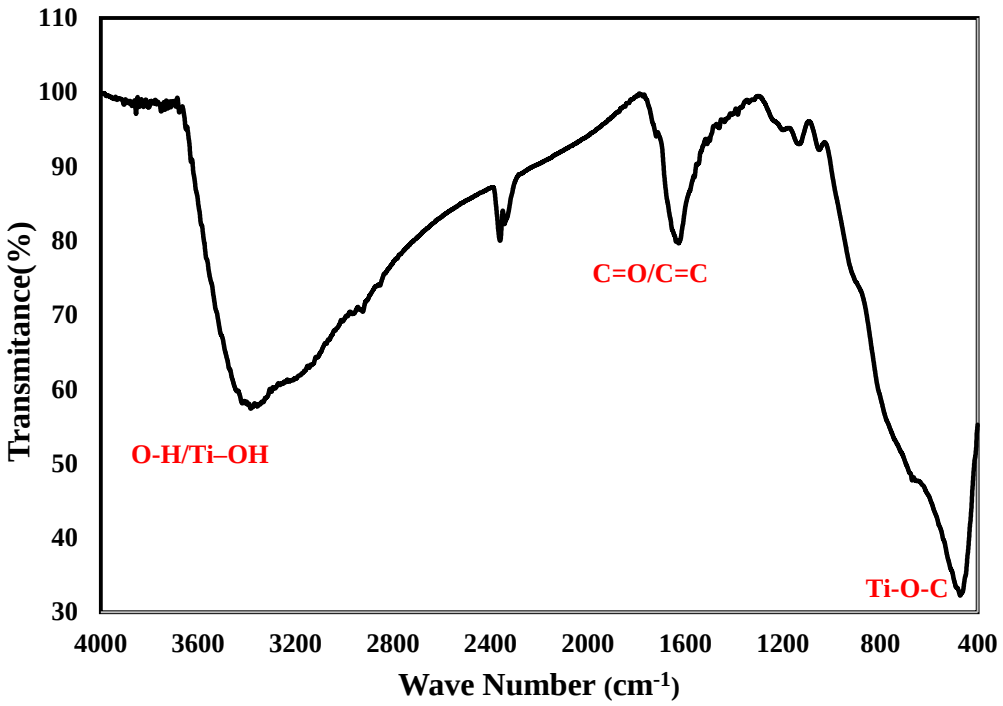

Figure 4.8 FTIR spectra of TiO_2-GO compound.

4.1.4 Scanning Electron Microscopy (SEM)

The morphology of TiO_2-GO compound was investigated using a field-emission scanning electron microscope (FESEM). SEM images of TiO_2-GO compound are shown in figure 4.9. As can be visualized, TiO_2 particle formation is exhibited on the surface of GO nanosheets by the white color. The derived TiO_2 particles could be stuck into the GO nanosheets by hydrogen bonding. As noted, the graphene structure prevents the accumulation of TiO_2 particles on the GO nanosheets and ensures a good distribution of TiO_2 particles on GO nanosheets [80], [81]. Energy dispersive X-ray (EDX) was applied for TiO_2-GO compound (figure 4.10), to prove the presence and well dispersion of titania particles on GO layers. As shown, the titanium element (Ti) is present in the TiO_2-GO

compound which proves the successful synthesis of the compound. Besides, it can be seen from the mapping of Ti in figure 4.11 that TiO_2 particles are uniformly dispersed on GO nanosheets without any agglomeration.

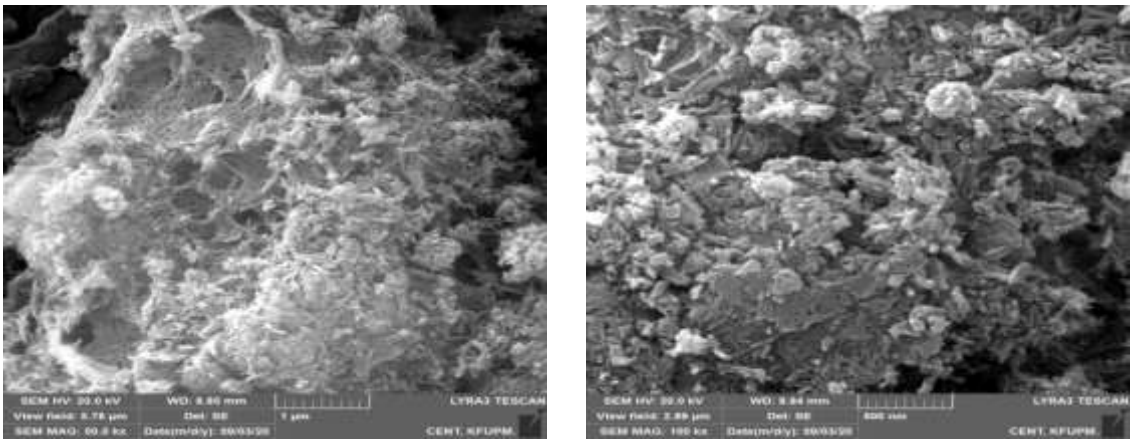

Figure 4.9 SEM images of TiO_2-GO compound.

Table 4.1 Weight composition of TiO_2-GO elements.

Element	Weight %
C k	14.62
O k	56.5
Ti k	28.88
Totals	100.00

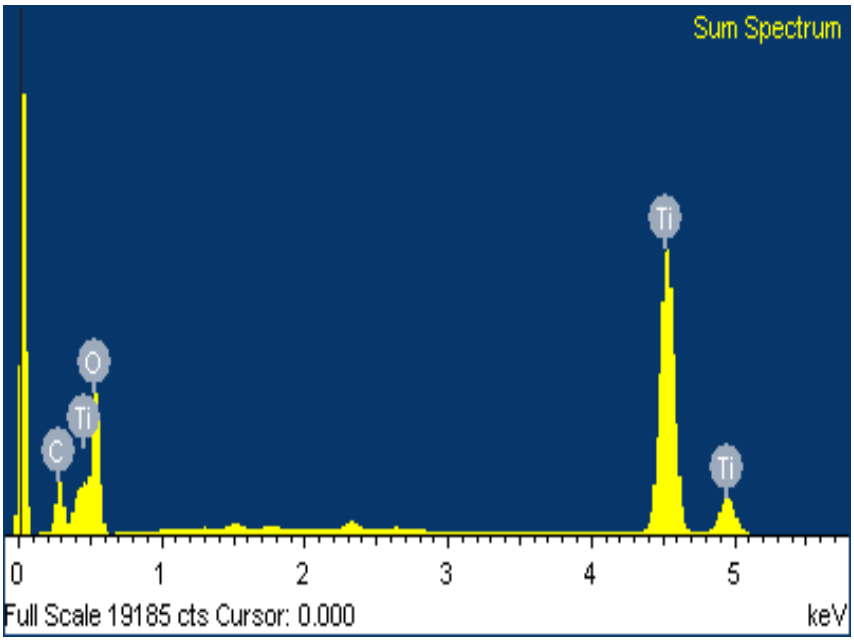

Figure 4.10 EDX of TiO_2-GO compound.

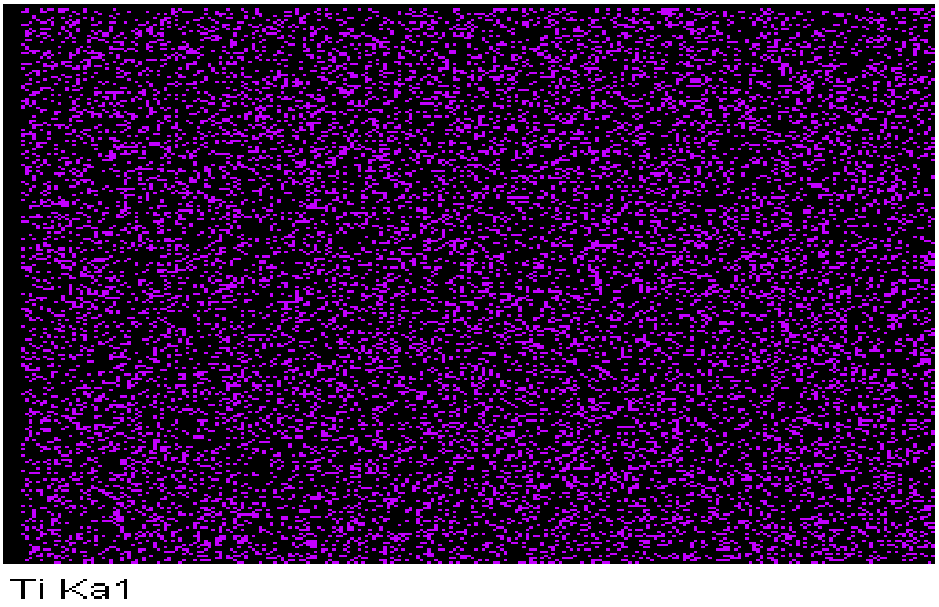

Figure 4.11 EDX mapping of Ti element in TiO_2-GO compound.

4.2 TiO_2-GO Membrane Characterization

4.2.1 X-Ray Photoelectron Spectroscopy (XPS)

XPS is performed to analyze the atomic concentrations and element types, which can illustrate the presence of layers on the surface of PA membrane. XPS is also applied to the modified membranes after the filtration testing to represent the binding durability of the embedded nanoparticles, even after the harsh operating conditions. The XPS scans of the modified membrane before filtration testing are shown in figures 14.12-14.15. As depicted, the C 1s spectrum shows four peaks. The first peak at around 284.6 eV is associated with C-C and C=C bonds. The second peak seen at about 285.8 eV is related to C-O bonds. The other two peaks exhibited at around 287.1 eV, and 289.4 eV are linked to C=O and O-C=O bonds respectively [71], [82], For the titanium spectrum(Ti 2p), the peak indicated at about 447.2 eV is ascribed to Ti $2p_{3/2}$. In addition, another peak appeared at around 458.5eV is corresponded to Ti $2p_{1/2}$ [83]. O 1s spectrum displays a peak at about 532.4 eV which is attributed to C=O bonds and another peak depicted at around 533.8 eV that is ascribed to C-O bonds[84]. The XPS spectra of the modified membrane after filtration testing are depicted in figures 14.15-14.19. The C 1s spectra represent two peaks around 284.9 eV and 285.9 eV ascribed to C-C and C-O respectively [84], [85]. The titanium (Ti 2p) spectrum has a peak at about 453.3 eV related to Ti $2p_{3/2}$ and another peak at approximately 459.2 attributed to Ti $2p_{1/2.}$ The signals of Ti $2p_{3/2}$ and Ti $2p_{1/2}$ have a chemical state of Ti^{4+} [86]. It can be observed that there is increase in the binding energy after the filtration testing compared to before filtration case and this can be explained by the presence of other elements on the surface

produced by the filtration process. These elements can result in a decrease in the electron density around the coating elements and lead higher binding energy. The peaks of O 1s are displayed at around 531.6 eV and 532.8 eV that are attributed to C=O/O=C-O and C-O respectively [84]. As noted, the same elements are appeared in the XPS of the modified membrane before and after filtration testing. The binding energies of the elements in both cases are also approximately similar to each other. This can prove that the added nanoparticles are strongly adhered to the membrane surface and not affected by the harsh conditions of the filtration testing. The XPS analyses of modified membranes before and after filtration testing provide the presence of titanium (Ti) elements in the coated membranes by showing their peaks.

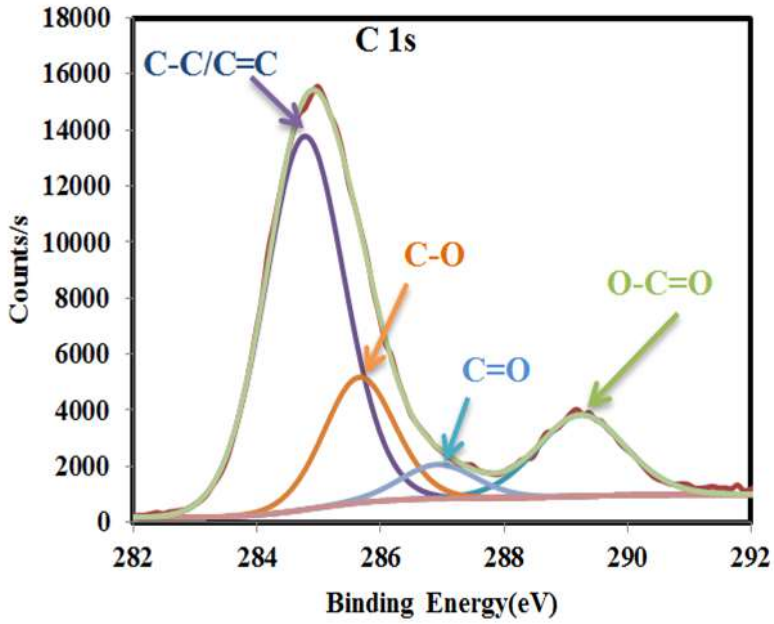

Figure 4.12 XPS C 1s spectra of the modified membranes before testing.

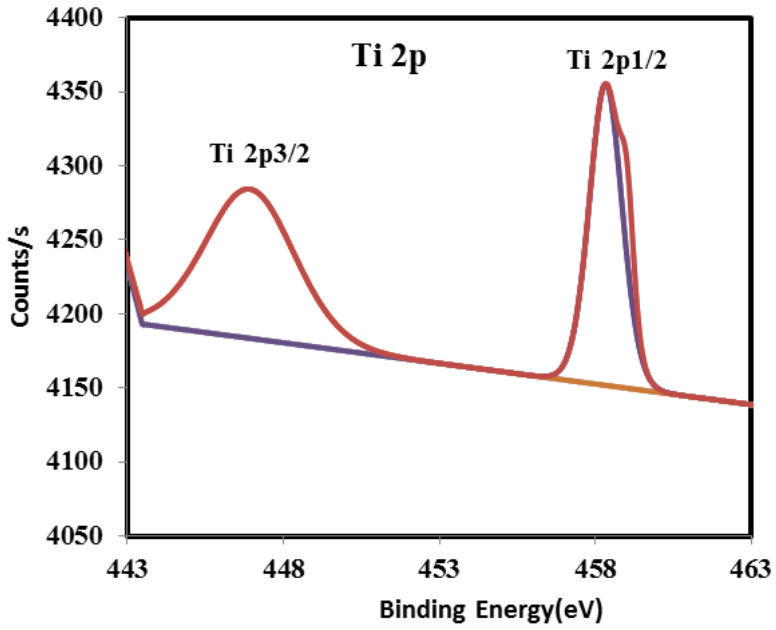

Figure 4.13 XPS Ti 2p spectra of the modified membranes before testing.

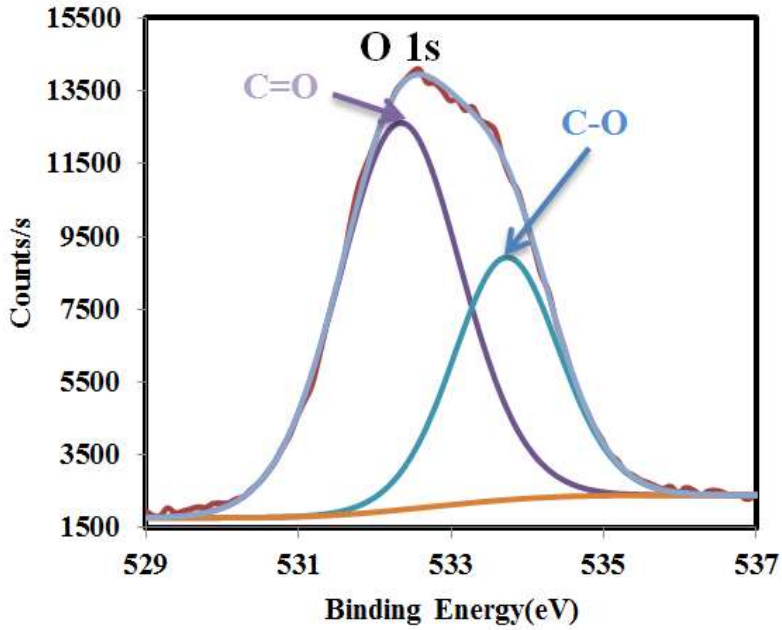

Figure 4.14 XPS O 1s spectra of the modified membranes before testing.

.

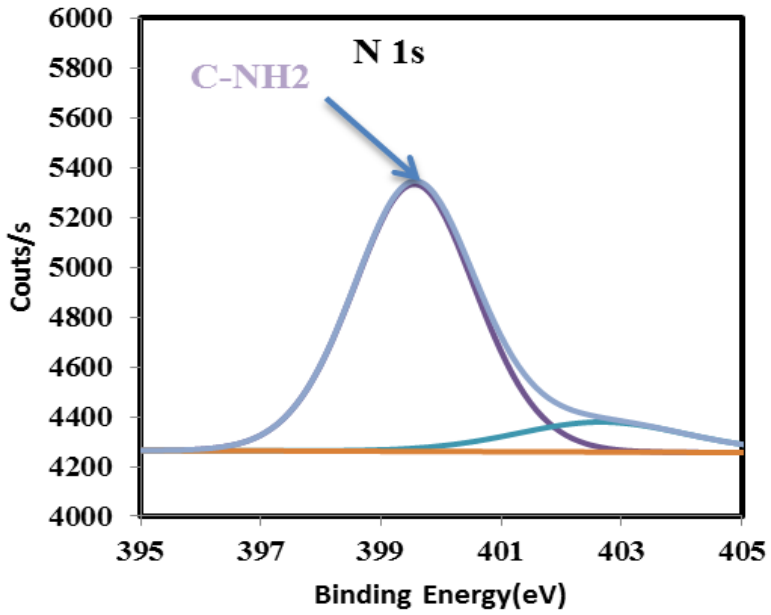

Figure 4.15 XPS N 1s spectra of the modified membranes before testing.

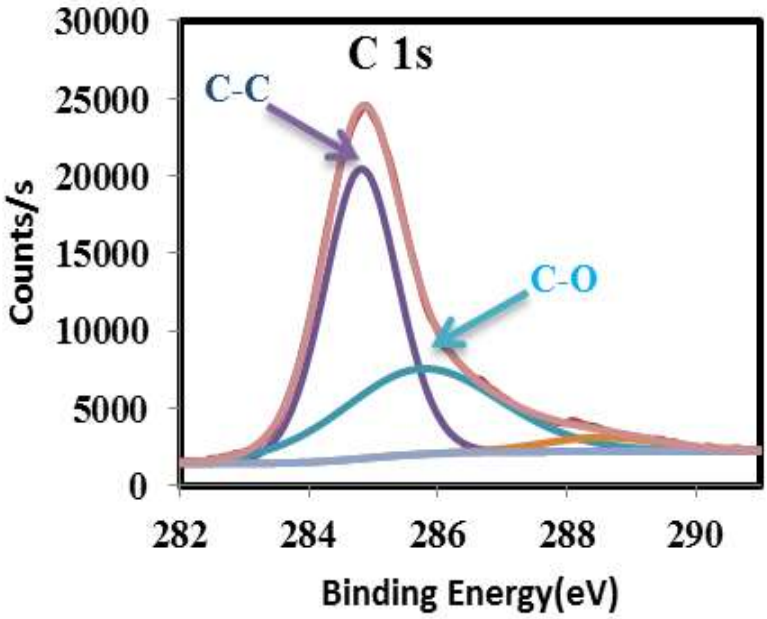

Figure 4.16 XPS C 1s spectra of the modified membranes after testing.

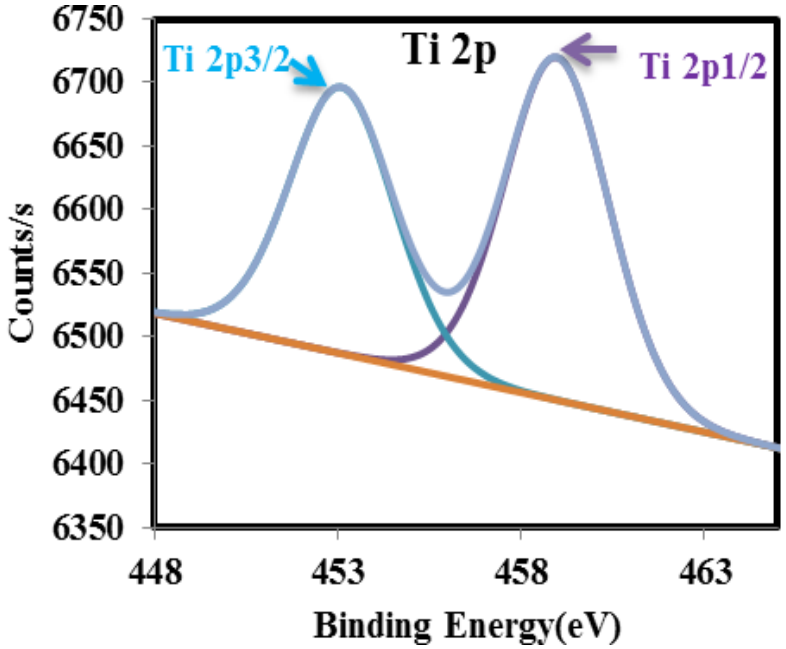

Figure 4.17 XPS Ti 2p spectra of the modified membranes after testing.

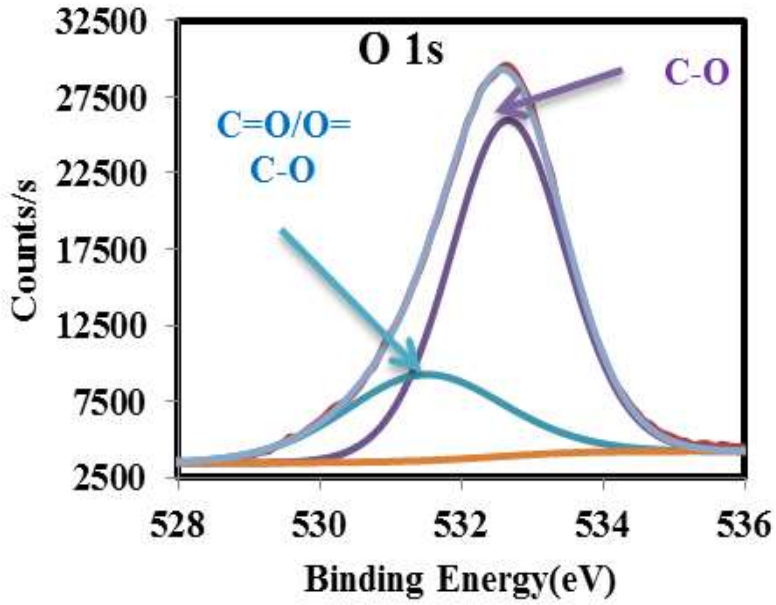

Figure 4.18 XPS O 1s spectra of the modified membranes after testing.

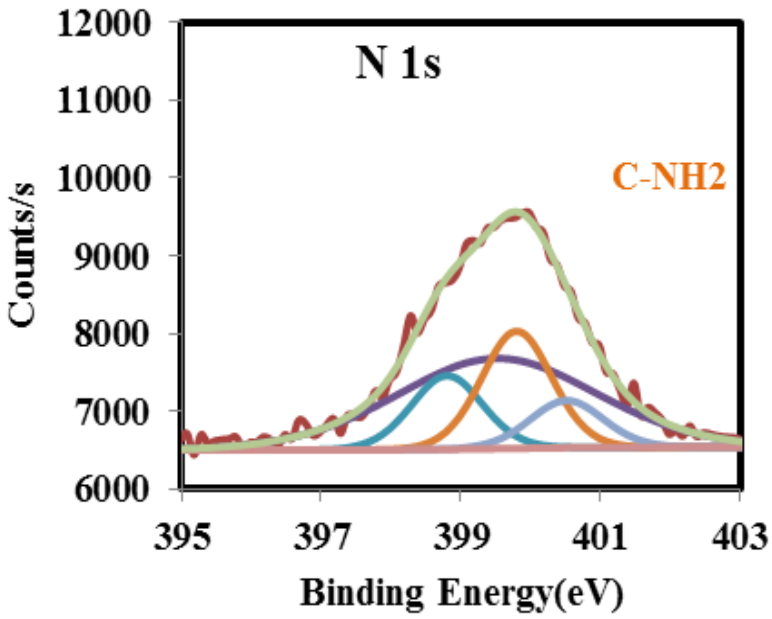

Figure 4.19 XPS N 1s spectra of the modified membranes after testing.

4.2.2 Fourier Transform Infra-Red (FTIR)

To approve the presence of TiO_2 -GO compound on the surface of the membrane and analyze its present functional groups, FTIR analysis was performed on the modified membrane. Figure 4.20 depicts the FTIR spectra of the TiO_2 -GO compound PA membrane. A broad peak observed at around 3420 cm^{-1} is ascribed to the stretching vibrations of the hydroxyl group (O-H). This specific group indicates the compound dispersion on the membrane which makes it a more hydrophilic surface [87]. Moreover, The peak demonstrated near 2925 cm^{-1} is related to the stretching of the C-H and aliphatic O-H groups of the polyamide [88], [89]. The absorption band exhibited near 1630 indicates the stretching vibration of aromatic C=C bonds and the bending vibration of the water molecule(OH) [70]. Besides, The peak seen around 1535 cm^{-1} is associated with the N-H bending vibration and the stretching vibration of C-N bonds [90]. The

membrane also shows a peak near 1065 cm^{-1} that can exhibit the stretching vibration of C-O bonds [70]. As shown, the absorptions that appeared at the range of 400-1000 cm^{-1} can be assigned to Ti-O-Ti bonds [91]. In addition, The noted shift of Ti-O-Ti bonds to about 790 cm^{-1} compared to TiO_2-GO denotes to the vibration of the combined signal of Ti-O-C and Ti-O-Ti [73].

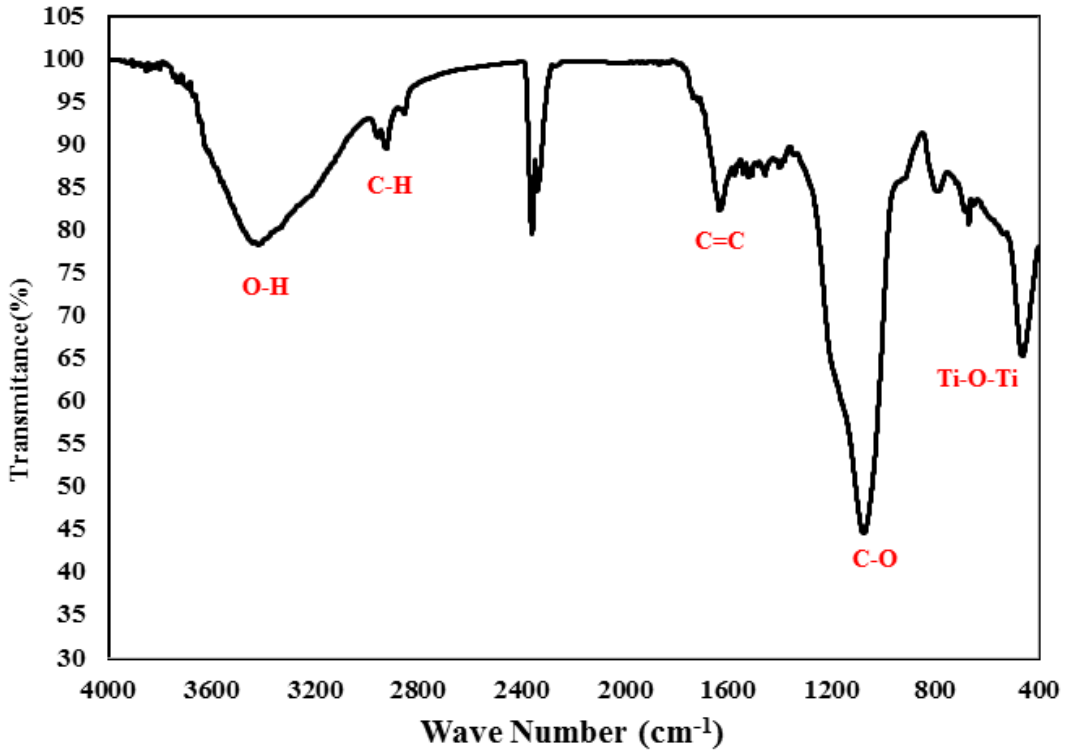

Figure 4.20 FTIR spectra of TiO_2-GO compound on membrane surface.

4.2.3 Scanning Electron Microscopy (SEM)

SEM was applied to look over the morphology (surface and cross-section) of the modified membrane. The surface SEM images of the PSf support, bare membrane (uncoated polyamide membrane), and modified PA membrane (coated with TiO_2-GO compound) are depicted in figures 4.21, 4.22 and 4.23 respectively. The SEM image of

PSf support as shown in figure 4.21 demonstrates the uniform and porous nature of the polysulfone layer. The bare membrane as represented in figure 4.22 shows the rough surface of the polyamide layer. In addition, the SEM images of the bare membrane indicate the typical morphology of the polyamide membranes formed by polymerization process of MPD and TMC which is known as ridge-and-valley structure[36]. The modified membrane SEM images as illustrated in figure 4.23 represent two different colors which indicate the dense PA layer and TiO_2-GO compound [88]. The observed morphology in SEM images of modified membrane exhibits the ridge and valley shape of MPD and TMC structure [36]. As can be noted, the embedded particles made the membrane surface denser and grainy structure [72], [73], [84]. The cross-sectional SEM was applied to identify the constituent layers of the membrane and roughly calculate their thickness. Cross-section SEM analysis of polysulfone support indicates asymmetric shape with approximately 110 μm thickness as depicted in figure 4.24. Moreover, a polyamide layer of about 300 nm thickness was formed on the polysulfone support as shown in figure 4.25. As can be seen in figure 4.26, incorporating the TiO_2-GO compound into the polyamide layer form a very thin film. As a result, it is not discernible in the image and it did not considerably affect the thickness of the PA layer. Polyamide and polysulfone layers can be easily recognized and distinguishable from each other because PSf layer has higher porosity whereas the PA layer is very dense and non-porous [36], [81].

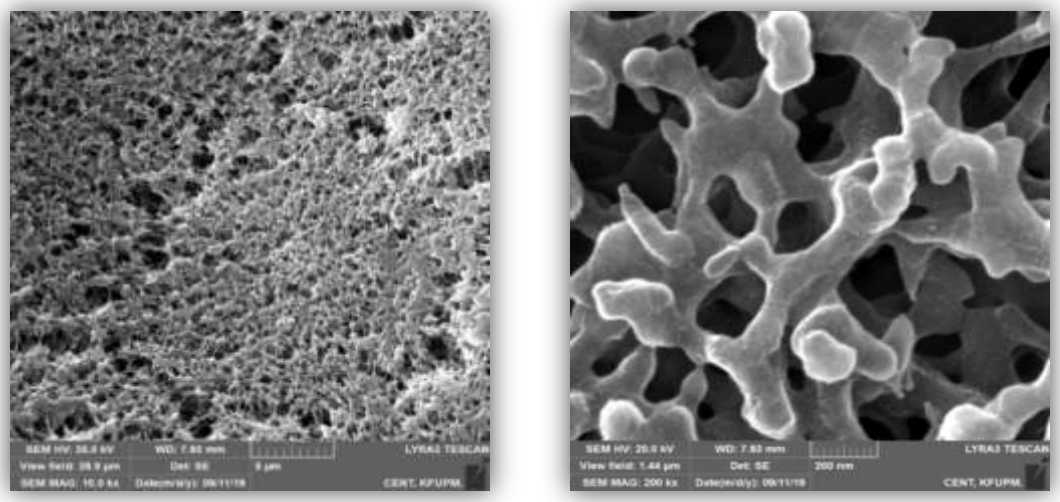

Figure 4.21 SEM images of the Polysulfone support showing its highly porous nature.

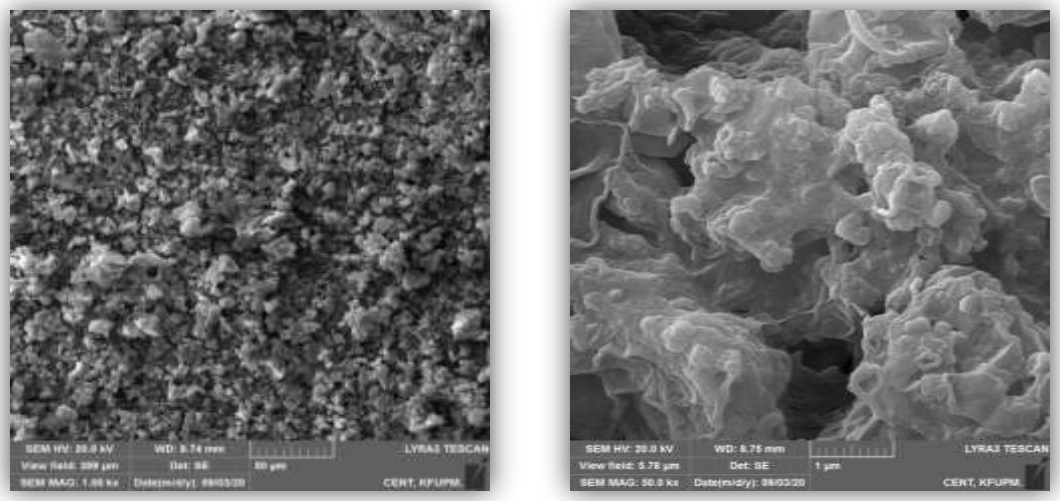

Figure 4.22 SEM images of the uncoated PA membrane depicting its typical morphology.

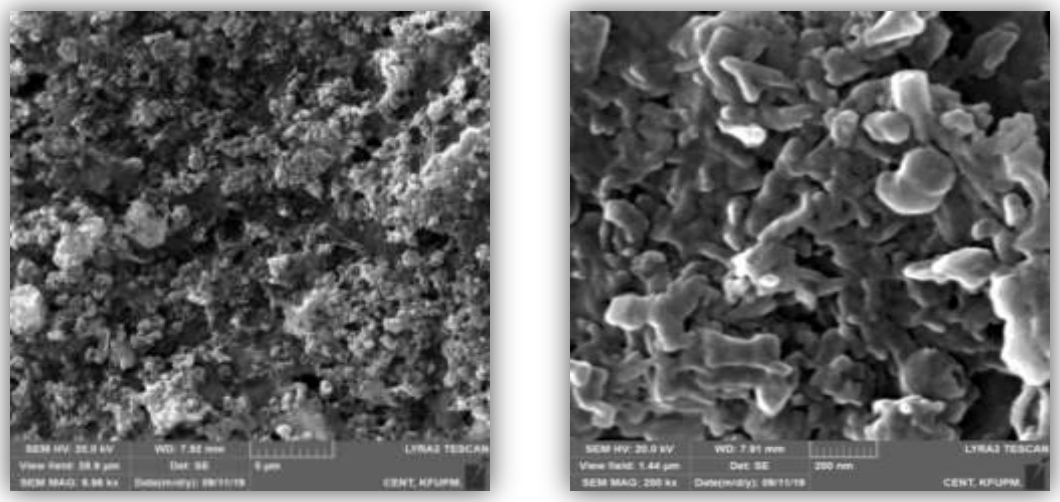

Figure 4.23 SEM images of the membrane coated with GO-TiO_2 compound.

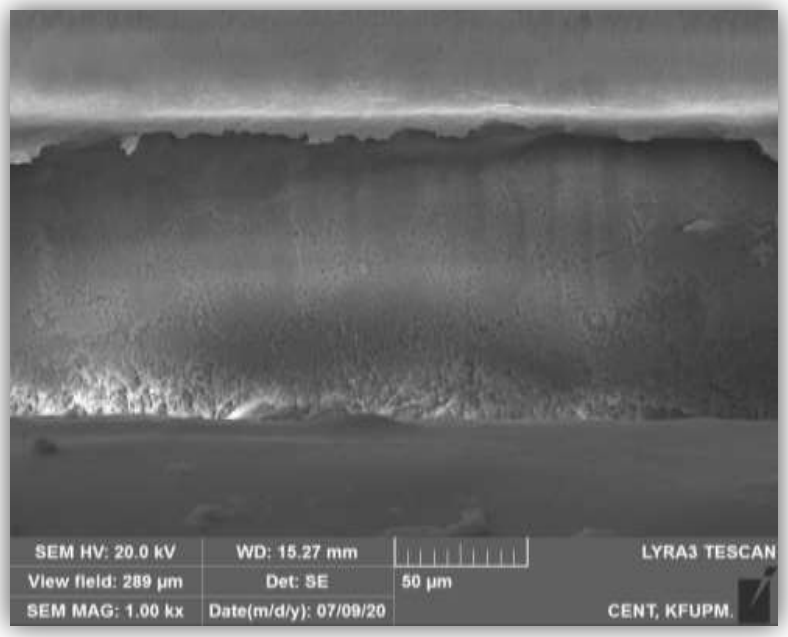

Figure 4.24 Cross-sectional SEM images of the Polysulfone support.

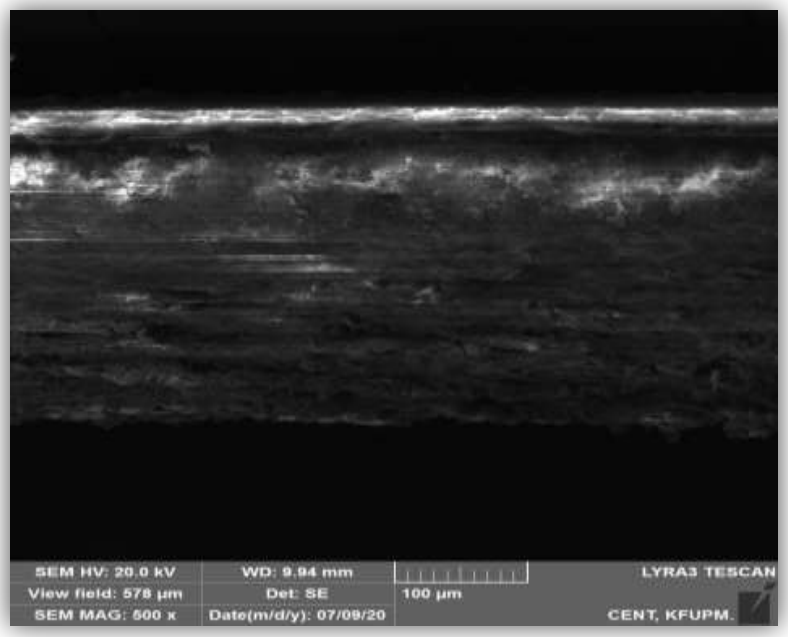

Figure 4.25 Cross-sectional SEM images of bare PA membrane.

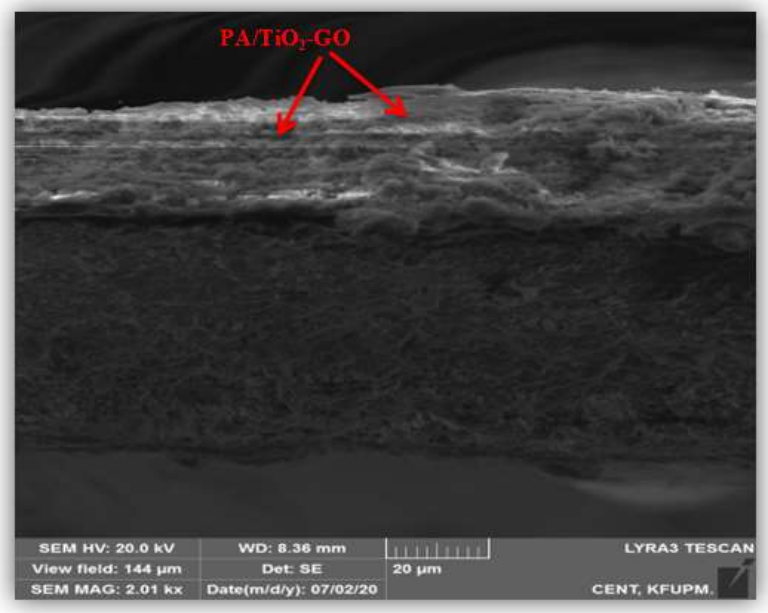

Figure 4.26 Cross-sectional SEM images of TiO_2 –GO/ PA membrane.

4.2.4 Energy-Dispersive X-Ray Spectroscope (EDX)

Energy-dispersive X-ray spectroscope (EDX) was used to analyze quantitatively the nanoparticles on the surface of membranes to confirm the presence and the good dispersion of TiO_2-GO compound on the membrane surface. As can be seen in figures 4.27-4.29, the different peaks shown reflect the presence of different elements. The one peak in figure 4.27 (polysulfone support) shows the presence of carbon. Moreover, figure 4.28 represents five peaks which indicate carbon, titanium, oxygen, nitrogen and chlorine elements present in the coated membrane before the filtration testing. The presence of the titanium (Ti) element in the EDX of the modified membrane confirms the presence of TiO_2-GO on the membrane surface. Figure 4.29 has six different peaks that depict the existence of carbon, oxygen, sodium, chlorine, titanium, and nitrogen on the surface of the coated membrane after the filtration testing. The appearance of elements before and after the filtration testing proves that the nanoparticles of TiO_2-GO are strongly adhered to the polyamide layer and not affected by the harsh conditions of the testing.

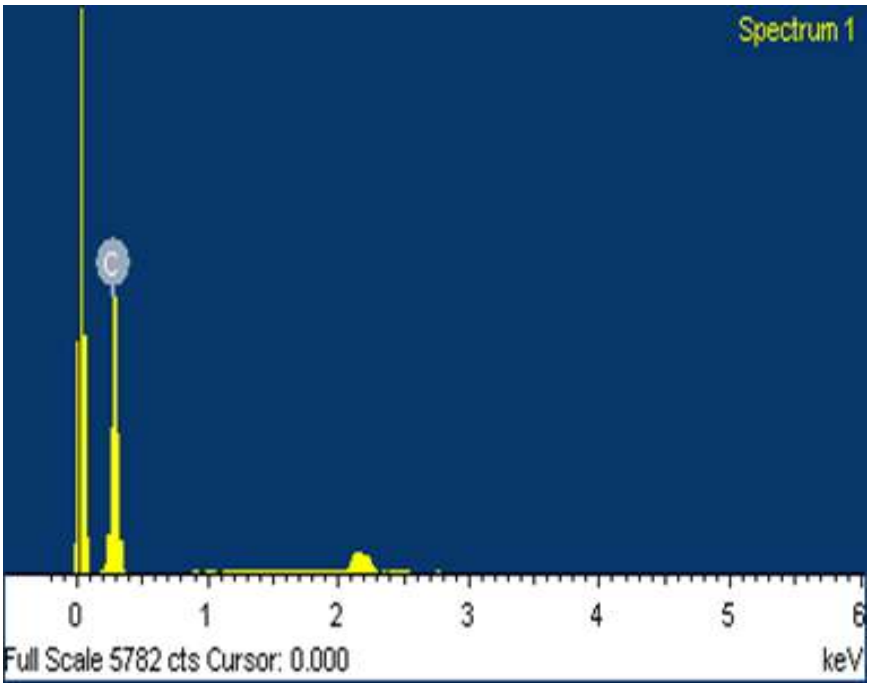

Figure 4.27 Results of EDX analysis for the Polysulfone support.

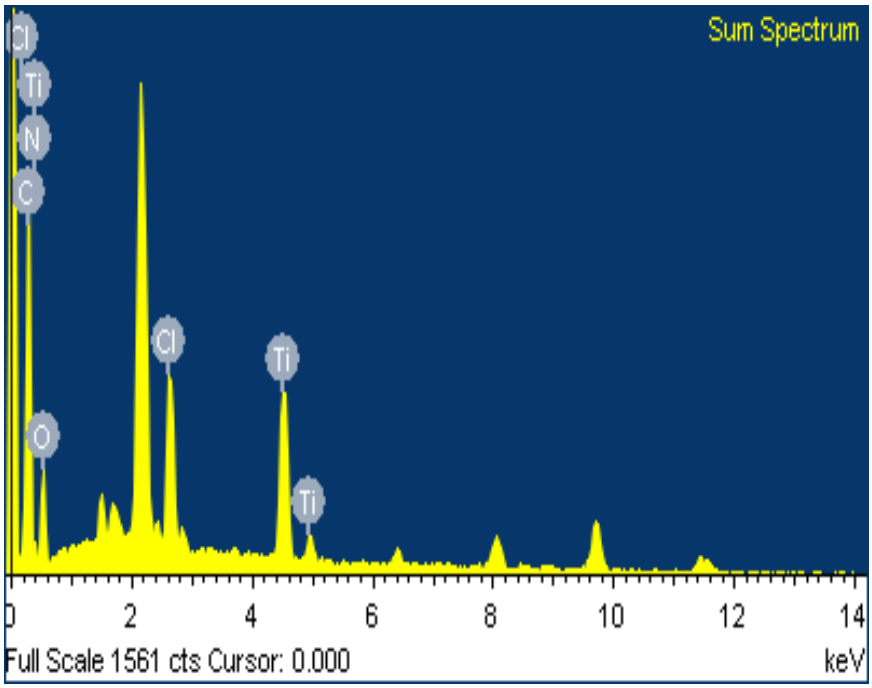

Figure 4.28 EDX analysis of the coated membrane before testing.

Table 4.2 Weight composition of the coated PA membrane elements before testing

Element	Weight %
C K	53.29
O K	24.18
N K	11.02
Cl K	4.06
Ti K	7.45
Totals	100.00

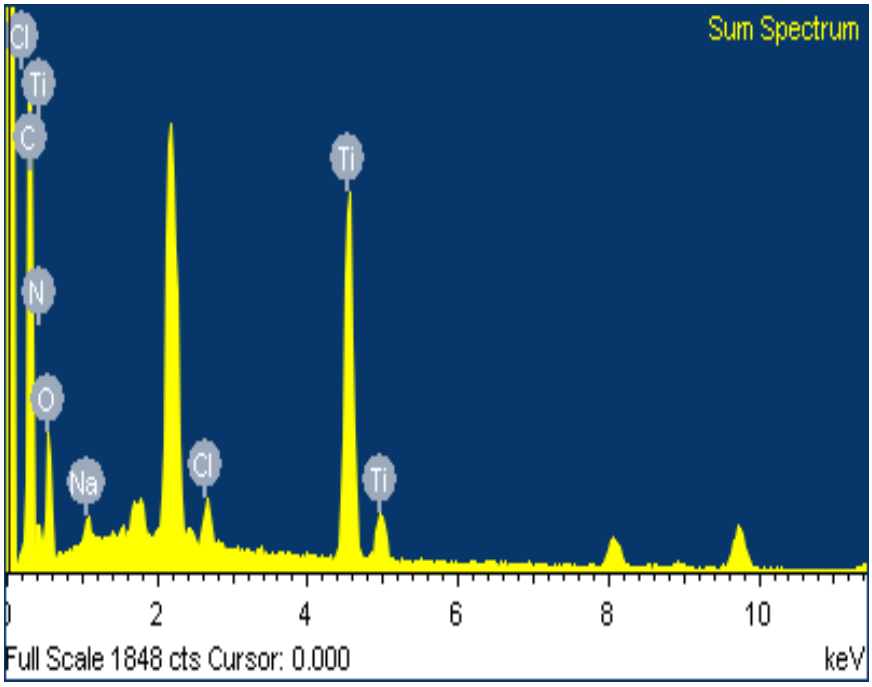

Figure 4.29 Results of EDX analysis for the PA membrane coated with TiO_2-GO compound after the filtration testing.

Table 4.3 Weight composition of the coated PA membrane elements after testing

Element	Weight %
C K	48.05
O K	29.47
N K	5.87
Cl K	1.06
Ti K	14.75
Na K	0.81
Totals	100.00

4.2.5 Atomic Force Microscopy (AFM)

AFM was used to evaluate the morphology of the thin-film composite membrane. Figures 4.30 to 4.32 shows the three-dimensional images of AFM for PSf support, bare (PA) membrane, and coated membrane. It is a more accurate method to map the surface roughness on the nanoscale. Table 4.4 represents the surface roughness variables of the membrane including average surface roughness (R_a), the difference in height between the highest crest and lowest valley (R_{max}), and the root means square roughness (RMS). As can be investigated, the bare (PA) membrane surface is the roughest surface. After

embedding TiO_2-GO nanoparticles into the pristine membrane, the surface roughness was clearly decreased. This proves that the surface of the membrane became smoother by incorporating the TiO_2–GO nanoparticles. This obviously shows that the nanoparticles are dispersed on the membrane surface and the ridge-and-valley structure of polyamide membrane surface filled by TiO_2–GO nanoparticles. In addition, the hydrogen bonds which are formed between the added nanoparticles and the polyamide layer [81], [92].

Table 4.4 Roughness parameters

Membrane Type	Ra(nm)	RMS(nm)	R_{max} (nm)
Support	33.6	45.8	347
Bare	37.6	51	402
Coated before testing	7.56	10.9	65.1

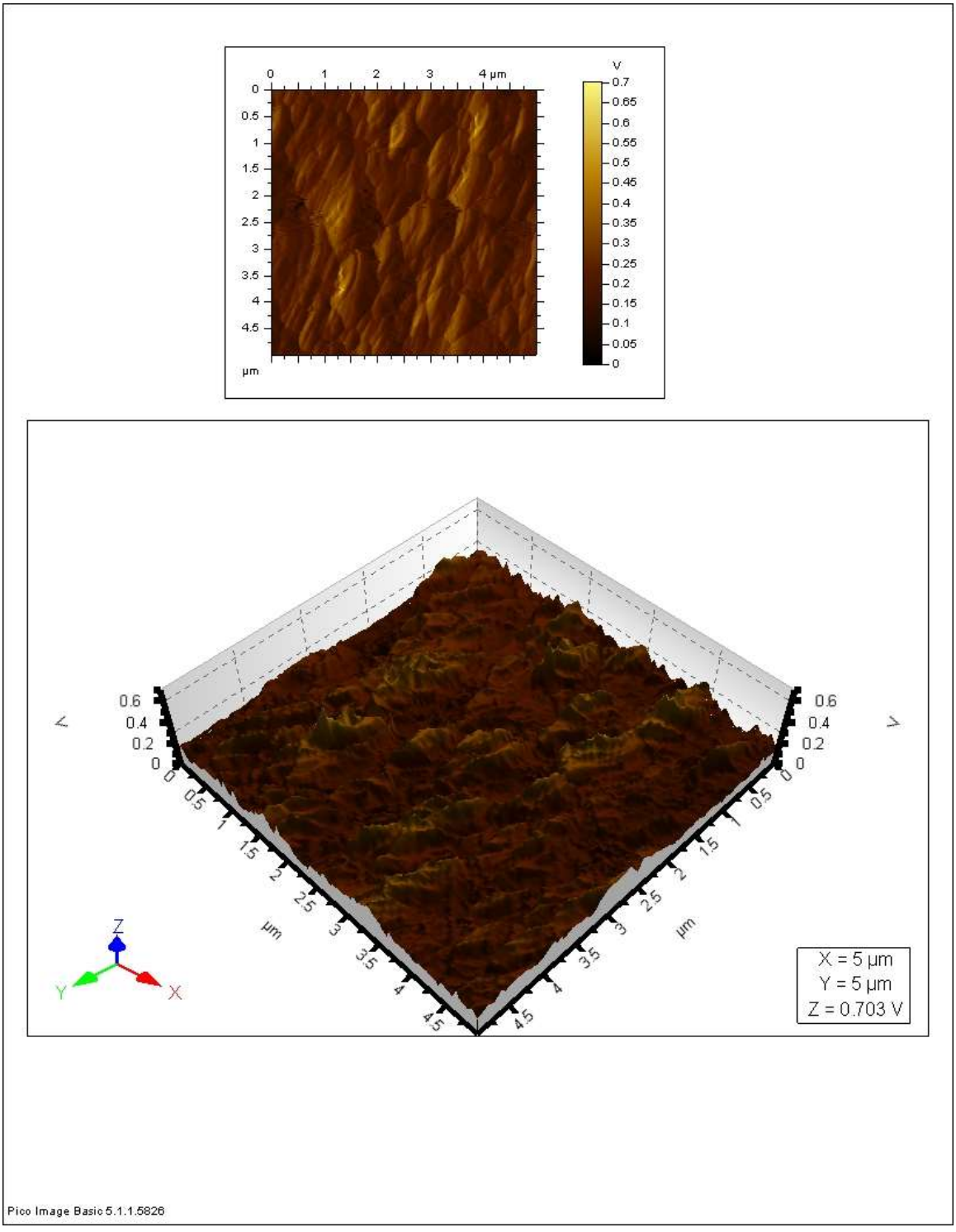

Figure 4.30 Three-dimensional AFM image of Polysulfone support.

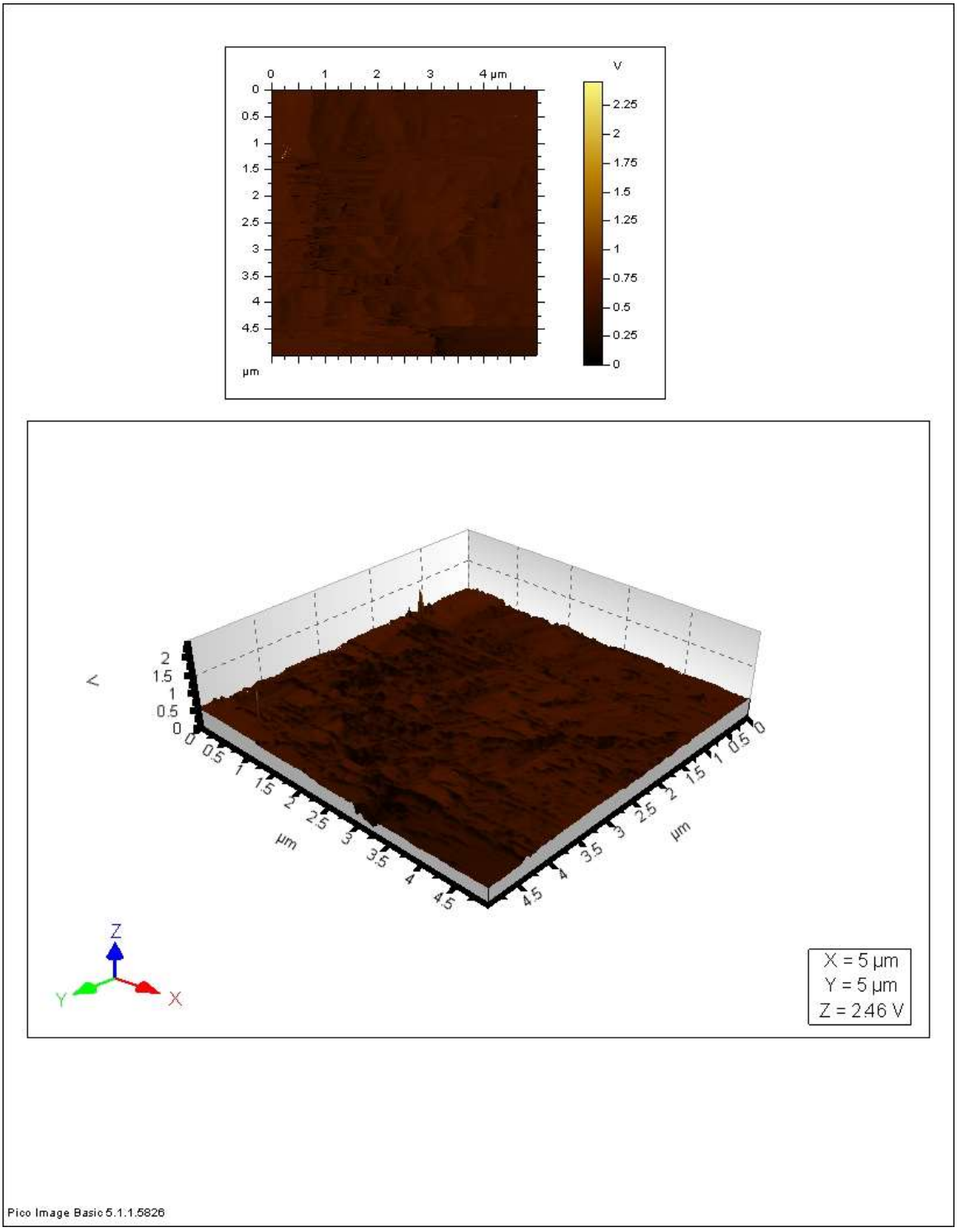

Figure 4.31 Three-dimensional AFM image of the bare membrane (PA).

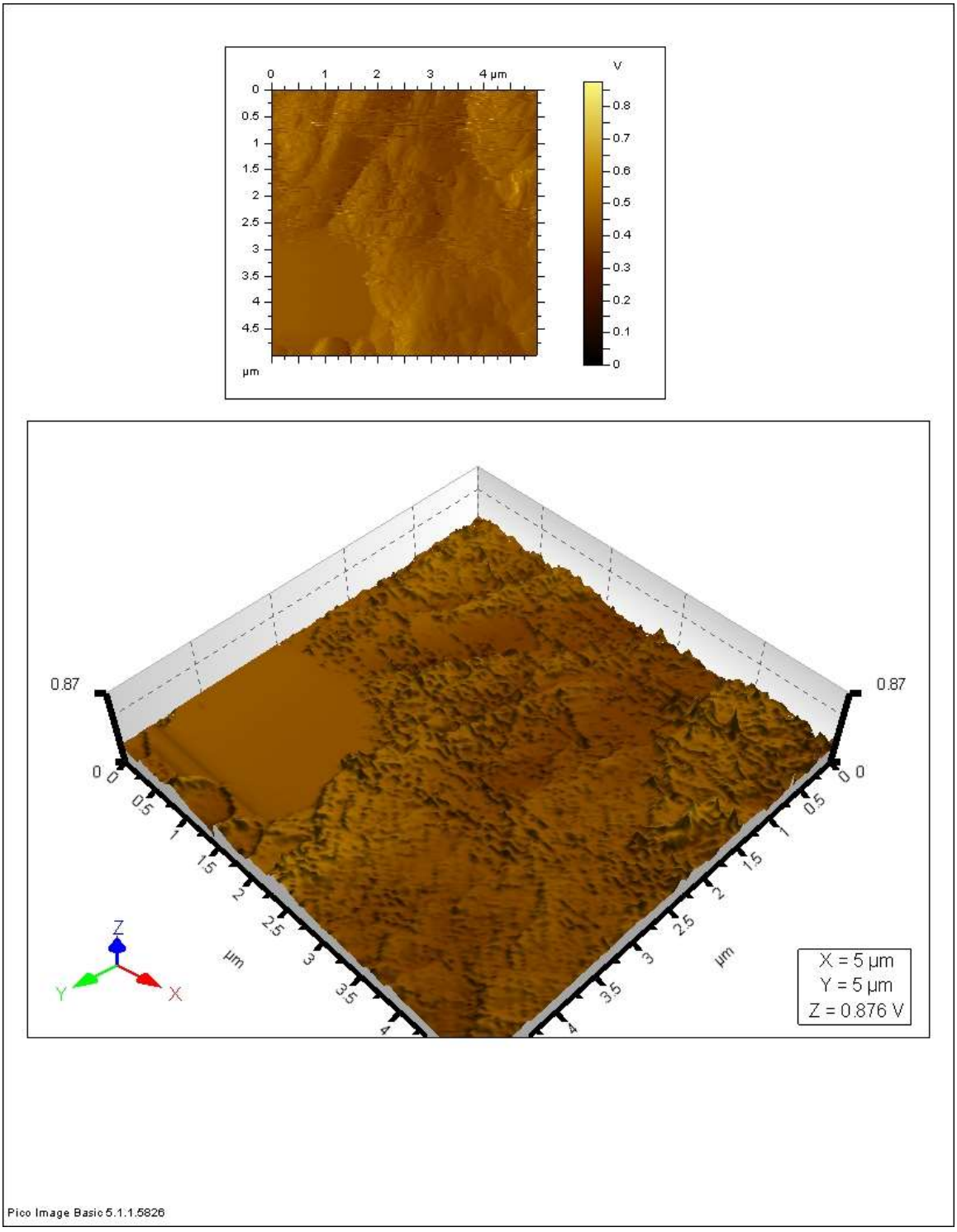

Figure 4.32 Three-dimensional AFM image of the coated membrane before testing.

4.2.6 Contact Angle Analysis

To study the wettability and hydrophilicity of the modified membrane surface, contact angle measurements are applied to the PSf support, bare membrane(uncoated PA membrane), and coated membrane of 8 layers. It can be obtained after the distilled water is dropped onto the membrane surface [93]. In general, lower contact angle values correspond to the high hydrophilicity of the tested surface. The contact angle values of the PSf support, bare membrane (uncoated PA membrane), and TiO_2-GO compound membranes of eight layers are depicted in figure 4.33. As can be seen, the contact angle values decrease from 79^o to 71^o and 53^o by TiO_2-GO compound incorporation. Membrane hydrophilicity was enhanced by adding TiO_2-GO because TiO_2-GO involves various functional groups that are of a partially negative nature which leads to higher hydrophilicity.

79°

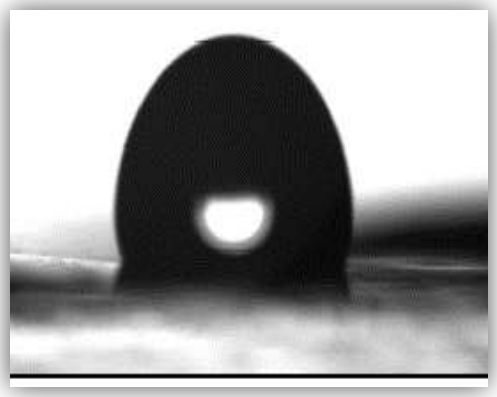

(a)

71°

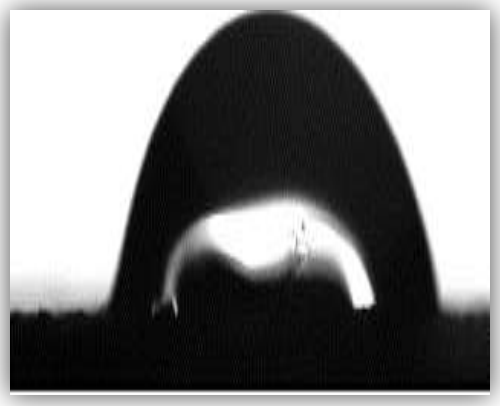

(b)

53°

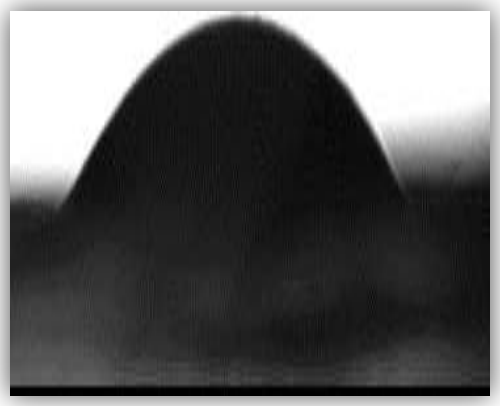

(c)

Figure 4.33 Contact angle of (a) support, (b) bare membrane, (c) coated membrane.

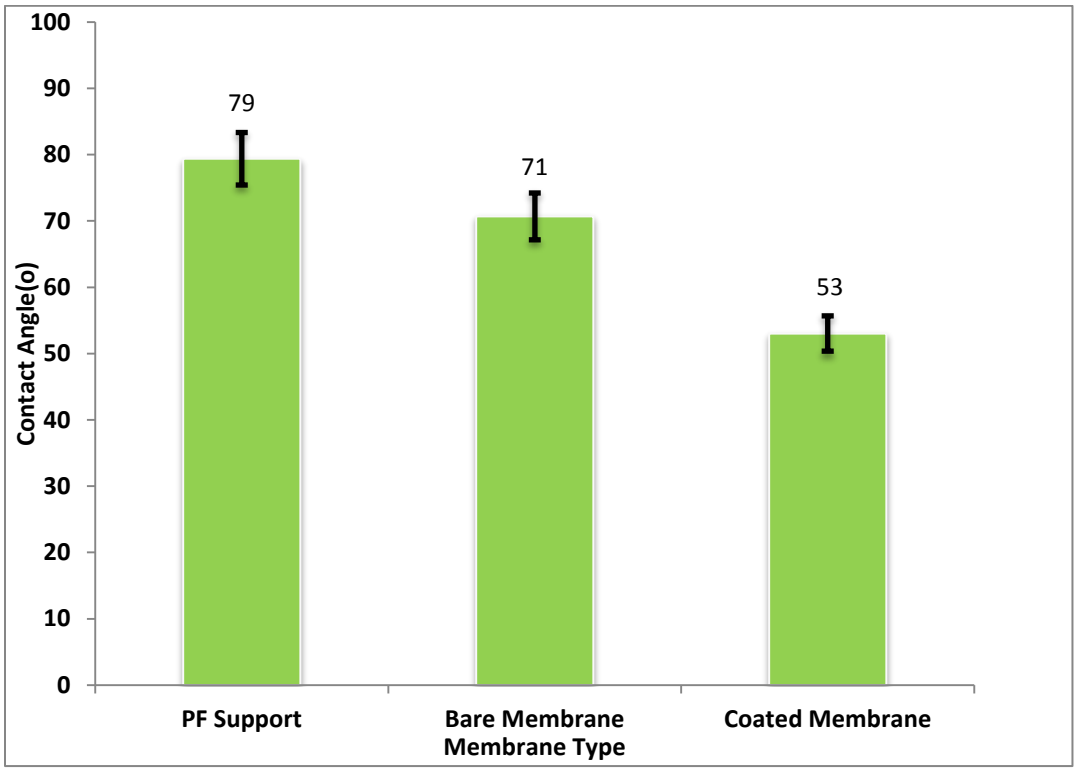

Figure 4.34 Bar chart of contact angles results of the prepared membranes.

4.3 Filtration Performance of Modified Membrane

4.3.1 Filtration Performance of the Modified Membrane at NaCl Solution

Filtration properties of the membrane have to be tested after each surface treatment because the membrane surface with another material adds an extra barrier layer to the permeate flux. It should be noted that if a modification of membrane surface results in a significant decline in flux (>30 %), then it is of no practical value [36]. To study the separation properties, the main output variables which attribute to the effectiveness and efficiency of performance (salt rejection and permeate flux) have to be maximized.

Almost all the surface modification ways found in the literature result in reducing the permeate flux. In most experiments, many researchers have noticed more than a 10 % decline in the permeate flux even at a very thin layer. However, during any surface modification, these two factors go in the opposite direction. If layer thickness increases, salt rejection increases and then making a high barrier for the permeate flux to pass. On the opposite side, if the film thickness decreases or the pores expand, the permeation will increase, and the salt will pass easily through the membrane leading to a sharp decline in the rejection. The permeate flux and salt rejection are the main parameters that determine the efficiency of the membrane in the purification of salty water. Therefore, it is very significant to analyze them. The rejection of NaCl, Na_2SO_4, and several hydrocabons were investigated for the modified membrane of different layers. The permeate flux was tested at NaCl and Na_2SO_4 solutions as shown in figure 4.35 and 4.36. The average permeate flux of the bare membrane is about 40 L/m^2h at a pressure of 1 MPa and an ambient temperature. It is noteworthy that the permeability of the coated membrane is superior compared to the pristine membrane. The water flux is improved by increasing the TiO_2-GO layers and its maximum value (~ 60 L/m^2h) is achieved at eight layers. The flux increase is about 50 % greater than the bare membrane. This enhancement in the permeate flux can be attributed to the increase in the hydrophilicity of the membrane surface by embedding TiO_2-GO compound. The hydrophilicity is significantly improved due to the high hydrophilic functional groups present on the TiO_2-GO compound and the high affinity of titania particles to water. It is known that the improved hydrophiliity of the surface increases the membrane permeability by attracting water molecules into the membrane matrix and easing their permeation[54], [81].The increase in the permeability

can be attributed to the increase in the interlayer spacing of the graphene oxide nanosheets when adding the titania particles. Larger interlayer spacing leads to lower resistance to water flow, therefore, improving the permeate flux [94].The NaCl rejection for the modified membrane with different layers is shown in figure 4.35. It is clear that the salt rejection of coated membrane is enhanced well by increasing the layers. As can be noted, the optimum NaCl rejection of the modified membrane was obtained at 8 layers. High rejection of Cl^{-1} in 8 layer membranes is indicating that there is a high electrostatic repulsion forces between the ions of chlorine and the surface of the membrane. These strong repulsion forces are related to the membrane where the high molecular weight in 8 layers membrane compared to 4 and one layer membranes increases the negative charges of the surface of membrane. Therefore the electrostatic repulsion between membrane surface and the solution ions increase producing higher salt rejection rate compared to other membrane.

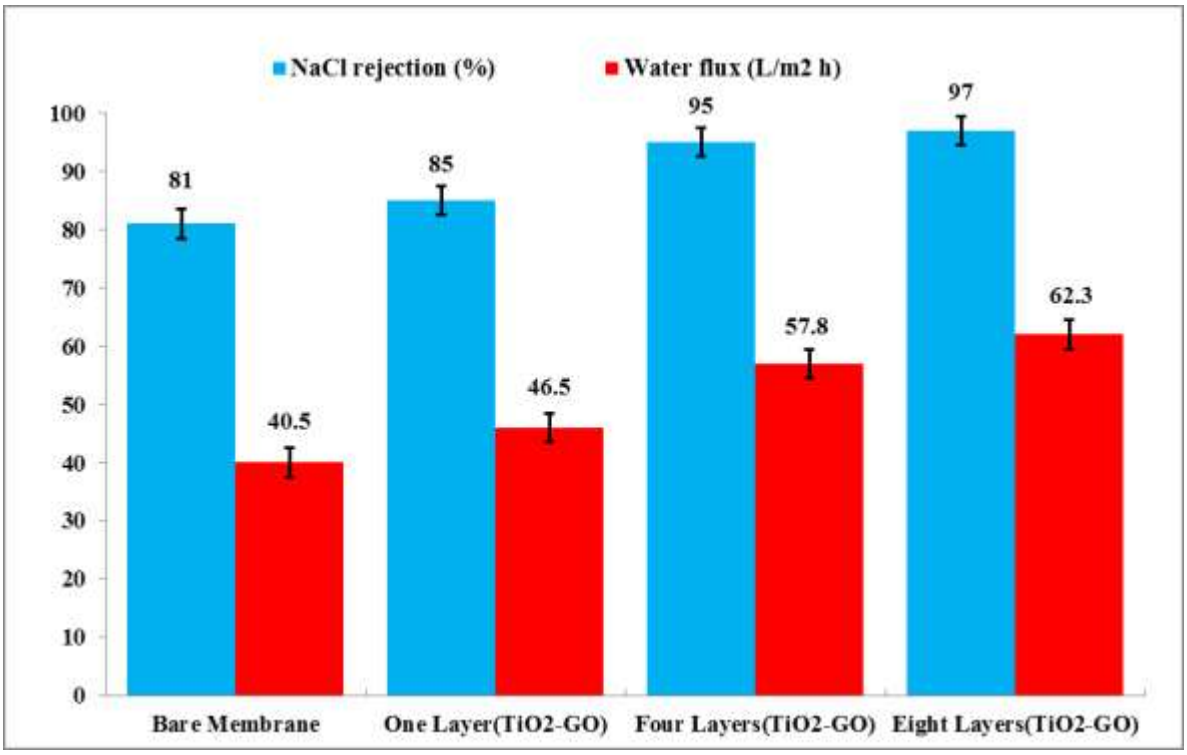

Figure 4.35 NaCl rejection and water flux of coated membrane with different layers.

4.3.2 Filtration Performance of the Modified Membrane at Na_2SO_4 Solution

In a similar method to that of NaCl solution, the Na_2SO_4 salt rejection of the membrane was tested. As shown in figure 4.36, it was significantly improved by adding TiO_2-GO compound into the polyamide membrane. The modified membrane showed superior performance in rejecting Na_2SO_4 at eight layers of TiO_2- GO compound which was 97 %. As can be realized, the rejection of Na_2SO_4 salt is generally greater than NaCl salt. This can be attributed to the attraction forces between divalent ions (SO_4^{2-}) and the surface of the membrane are very large compared to those between monovalent ions (Cl^-

) ions and membrane surface that prefers the sulfate permeation. In addition, the hydrated sulfate size is about 50% greater than the size of chlorine ions [95]. From the salt rejection results, it can be concluded that the modified membrane with eight layers is the optimum one.

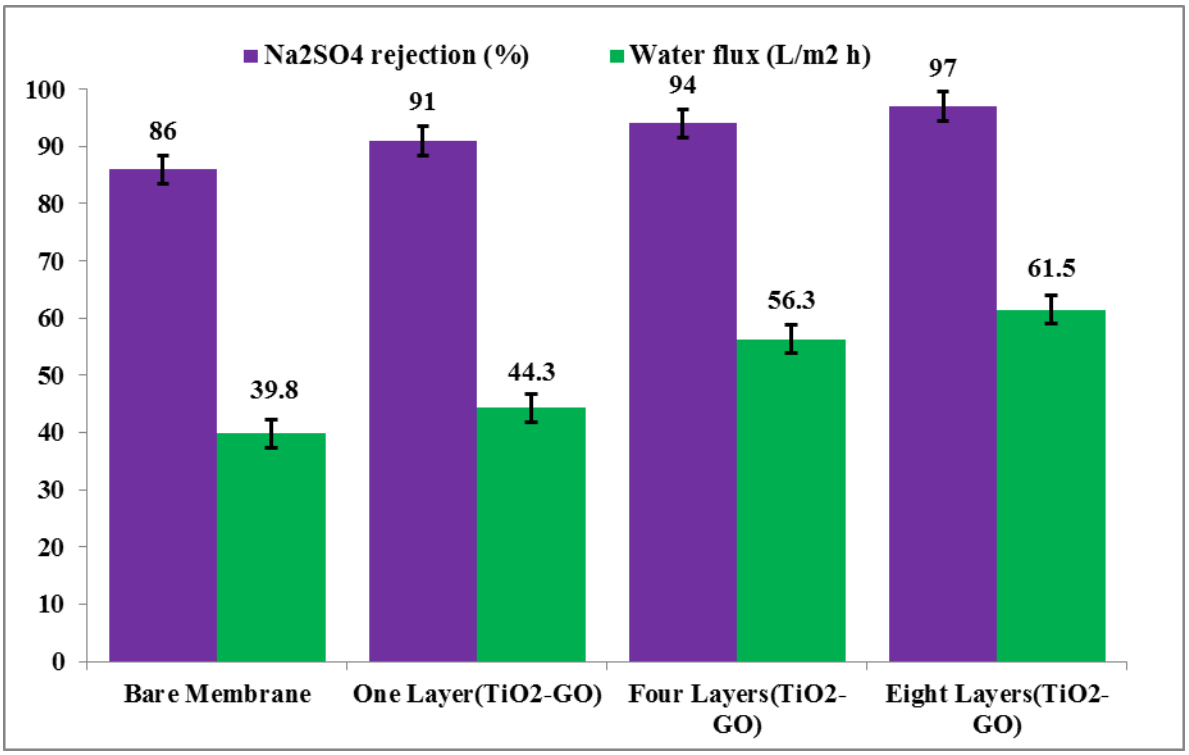

Figure 4.36 Na_2SO_4 rejection and water flux of coated membrane with different layers.

4.3.3 Filtration Performance of the Modified Membrane at Hydrocarbons Solution

To prove that the modified membrane can be used for desalination and seawater contaminated with oil, and to confirm that it can be efficient in organic molecule separation, the hydrocarbon rejection testing was applied to the optimum modified

membrane. The rejection of several hydrocarbons including toluene, dodecane, isooctane, and tridecane of the bare and modified membranes are shown in figure 4.37. The optimum modified membrane in permeability and salts rejection exhibited an excellent performance in the removal of hydrocarbons as well. Hydrocarbons rejection was showed a powerful advantage in rejecting many hydrocarbons including toluene, dodecane, isooctane, and tridecane as represented in figure 4.37.The optimal hydrocarbons' rejection efficiency was measured to be approximately 100%. The high rejection produced can be attributed to the high adsorption ability of the coated surface and the large size of organic molecules compared to membrane pores size. The achieved superior performance of the coated membranes attributed to that GO/TiO_2 compound has high sorption ability to water molecules.

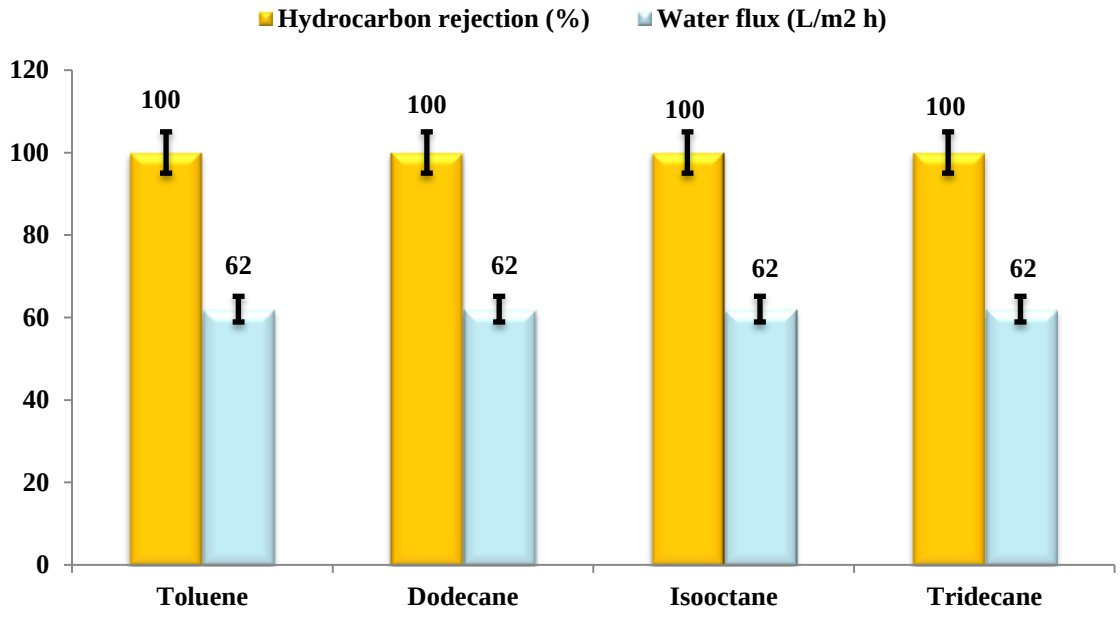

Figure 4.37 Hydrocarbons rejection of coated membrane with eight layers.

4.3.4 The Stability of the Optimum Modified Membrane

The mechanical and performance stability of the membrane is vital properties so they were evaluated. An experiment for measuring the membrane fluxes was applied for the optimally modified membrane at 1 MPa for 15 hrs. The fluxes of the modified membrane during 15 hrs are illustrated in figure 4.38. As shown, there is a gradual decrease of the membrane flux along the time and became stable after a certain time. This leads to that the formed active layer (consisting of the polyamide and GO-Titania nanoparticles) has excellent mechanical and performance stability. The observed minor flux decline in this testing can be associated with the rise in the operation temperature (around ~ 35 °C) that reduces the O/C ratio of the GO layers quickly during the long-term test [96]. The desirable stability of the coated membrane achieved during the long-term operation indicates the strengthened cross-linked structure and confirms that the GO-Titania membrane can be a promising candidate for real applications in water treatments.

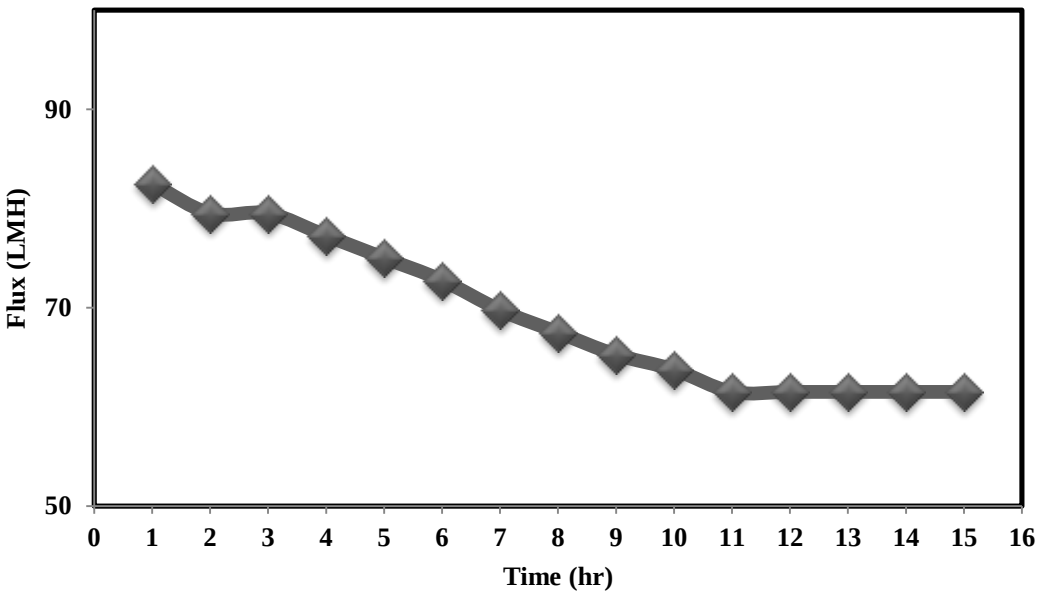

Figure 4.38 The study of the stability of the optimum modified membrane.

4.3.5 Layers and Feed Concentration Effects on the Filtration Performance of the Modified Membrane

The breakthrough of the modified membrane was studied by analyzing the effect of salt concentration of the feed and the number layers on the salt rejection. Figure 4.39 depicts the effect of salt concentration of the feed tank on salt rejection. As can be visualized, in the first stage the membrane works perfectly to completely reject the salts. Then, some salts penetrate with water indicating the breakthrough point. It can also be noted that the increase in the feed salt concentration resulted in a decrease in salt rejection of modified membranes. The high concentration of the salt increases the length of Debye of the electrostatic interaction between salt ions and membrane leading to high salt permeation through the membrane. Besides, the presence of a high concentration of salt causes the membrane swelling (expansion of polymeric membranes) which slightly expands the pore size and then eases the salt passage through the membrane. Another effect on permeability and salt rejection can be associated with the interactions of amine groups in MPD and acyl chloride groups in TMC. The effects of the number layers on the breakthrough point and salt rejection of the membrane are represented in figure 4.40. As shown, by increasing the number of membrane layers, the breakthrough took a longer time to appear. Increasing the layer thickness or density also produces high resistance to the salt passage thereby increasing the salt rejection percentage. As can be investigated, salt rejection is very low in one layer membrane because the PSf membrane has a poor hydrophlilicity (as shown in contact angle measurements) and one layer is not sufficient for producing membrane with desirable separation properties.

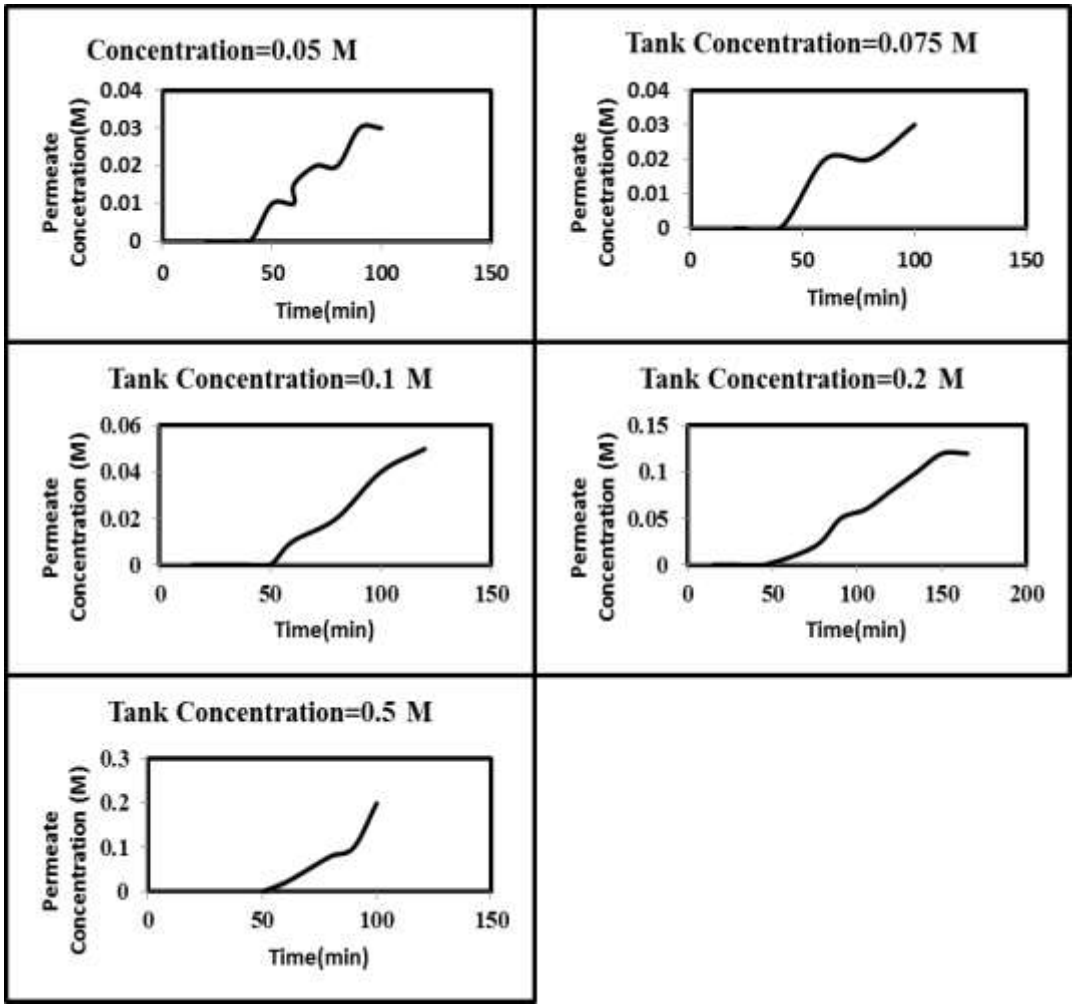

Figure 4.39 Feed concentration effect on the salt rejection of the membranes.

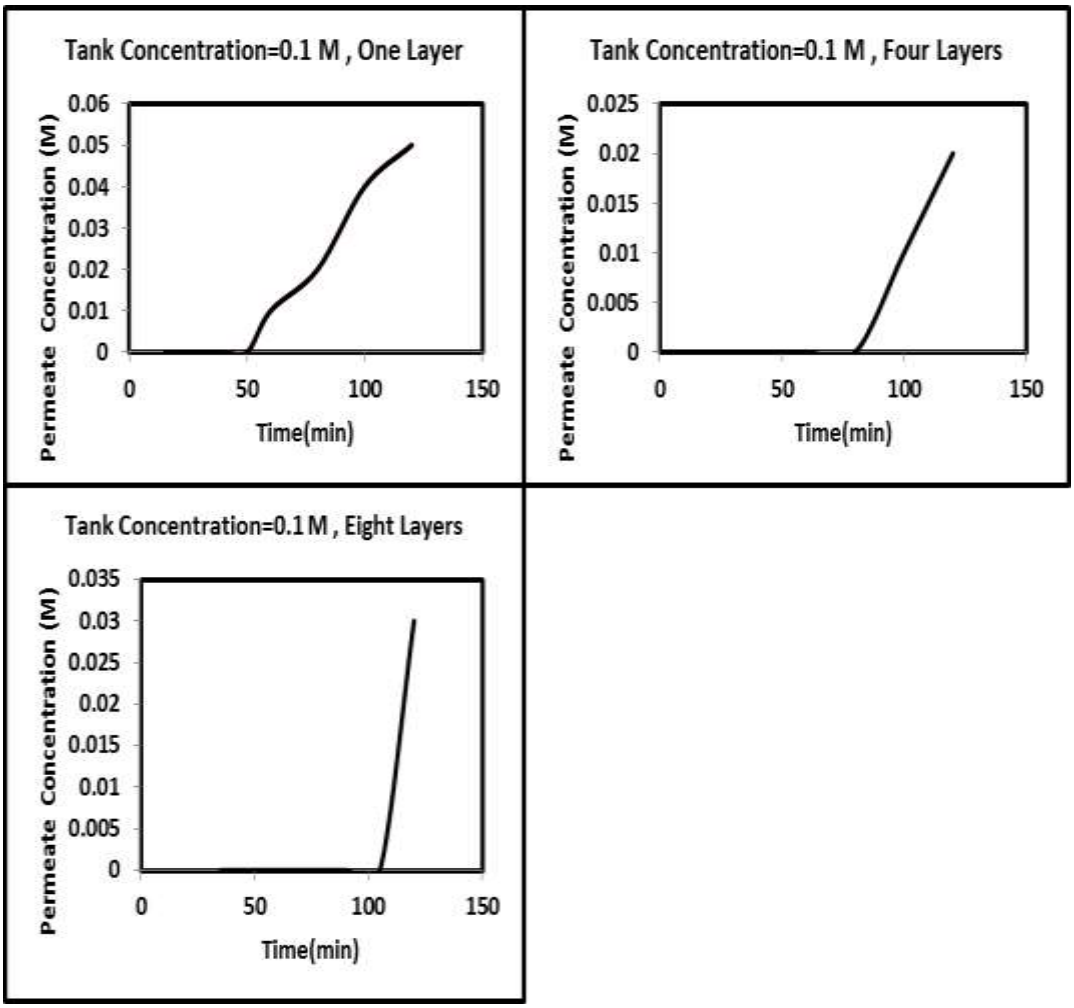

Figure 4.40 No. layers effect on the salt rejection of the membranes.

CHAPTER 5

CONCLUSIONS AND RECOMMENDATIONS

A novel inorganic compound (TiO_2-GO) was successfully synthesized using titanium tetraisopropoxide and graphene precursors. XRD results of the compound material showed that the titania is in the anatase phase and crystal structure. FTIR and XPS characterization of TiO_2-GO also indicated the presence of hydrophilic functional groups on the compound surface and successful chemical bonding between titania and graphene oxide. The modified polyamide membranes were successfully prepared by embedding the inorganic compound into the active layer over the polysulfone layer. The compound was incorporated into the polyamide matrix by dispersing it into the aqueous MPD. Different characterization techniques such as FTIR and XPS confirmed the presence materials on the membrane surface. SEM and AFM showed the typical morphology and the decrease of roughness after embedding the compound on the membrane surface. Moreover, contact angle measurements represented the hydrophilicity improvements after TiO_2-GO deposition on the membrane surface. Filtration testing of the modified membrane showed that the performance of the polyamide membrane has improved by embedding the TiO_2-GO compound in terms of salt rejection, hydrocarbons rejection, and water permeability. These improvements were obtained due to the increase in negative surface charge, hydrophilicity, and the surface roughness decline of the membranes. The optimum performance was achieved for the membrane with eight layers of TiO_2-GO including around 62 LMH permeate flux, 97 % salt rejection, and 100 %

hydrocarbons rejection. For ensuring that the modified membranes are much more reliable in the real application, the membranes should be tested under real conditions such as real seawater. Furthermore, the membrane can be tested under long-term experiment to make sure that the membrane can stand the higher temperature produced by the continuous higher pressure and check the fouling resistance at the same time.

REFERENCES

[1] T. Younos and K. E. Tulou, "Overview of desalination techniques," *J. Contemp. Water Res. Educ.*, vol. 132, no. 1, pp. 3–10, 2005.

[2] T. Younos and J. Lee, "Desalination: Concept and System Components BT - Corrosion and Fouling Control in Desalination Industry," V. S. Saji, A. A. Meroufel, and A. A. Sorour, Eds. Cham: Springer International Publishing, 2020, pp. 3–27.

[3] W. Graves, *Water: The Power, Promise, and Turmoil of North America's Fresh Water*. National Geographic Society, 1993.

[4] M. Xie, "Integrated Water Resources Management (IWRM) – Introduction to Principles and Practices 1," pp. 1–15, 2006.

[5] C. H. Tan, O. Lefebvre, J. Zhang, H. Y. Ng, and S. L. Ong, *Membrane Processes for Desalination : Overview*, no. June. 2012.

[6] M. Wilf and L. Awerbuch, *The guidebook to membrane desalination technology: reverse osmosis, nanofiltration and hybrid systems: process, design, applications and economics*. Balaban Desalination Publications, 2007.

[7] R. A. Tufa, G. Di Profio, E. Fontananova, A. H. Avci, and E. Curcio, "Forward Osmosis, Reverse Electrodialysis and Membrane Distillation: New Integration Options in Pretreatment and Post-treatment Membrane Desalination Process," in *Current Trends and Future Developments on (Bio-) Membranes*, Elsevier, 2019,

pp. 365–385.

[8] G. Kang and Y. Cao, “Development of antifouling reverse osmosis membranes for water treatment : A review,” *Water Res.*, vol. 46, no. 3, pp. 584–600, 2011.

[9] P. W. Morgan, *Condensation polymers: by interfacial and solution methods*, vol. 10. Interscience Publishers, 1965.

[10] M. Di Vincenzo, M. Barboiu, A. Tiraferri, and Y. M. Legrand, “Polyol-functionalized thin- fi lm composite membranes with improved transport properties and boron removal in reverse osmosis,” *J. Memb. Sci.*, vol. 540, no. June, pp. 71–77, 2017.

[11] A. Inurria *et al.*, “Polyamide thin- fi lm nanocomposite membranes with graphene oxide nanosheets : Balancing membrane performance and fouling propensity,” *Desalination*, vol. 451, no. July 2018, pp. 139–147, 2019.

[12] T. A. Otitoju, R. A. Saari, and A. L. Ahmad, “Journal of Industrial and Engineering Chemistry Progress in the modi fi cation of reverse osmosis (RO) membranes for enhanced performance,” *J. Ind. Eng. Chem.*, 2018.

[13] H. Organic, “Hybrid Organic / Inorganic Reverse Osmosis (RO) Membrane for Preparation and Characterization of TiO 2 Nanoparticle Self-Assembled Aromatic Polyamide Membrane,” vol. 35, no. 11, pp. 2388–2394, 2001.

[14] J. Kim and B. Van der Bruggen, “The use of nanoparticles in polymeric and ceramic membrane structures: review of manufacturing procedures and performance improvement for water treatment,” *Environ. Pollut.*, vol. 158, no. 7,

pp. 2335–2349, 2010.

[15] A. Rahimpour, S. S. Madaeni, A. H. Taheri, and Y. Mansourpanah, “Coupling TiO 2 nanoparticles with UV irradiation for modification of polyethersulfone ultrafiltration membranes,” vol. 313, pp. 158–169, 2008.

[16] M. Luo, J. Zhao, W. Tang, and C. Pu, “Hydrophilic modification of poly (ether sulfone) ultrafiltration membrane surface by self-assembly of TiO 2 nanoparticles,” vol. 249, pp. 76–84, 2005.

[17] A. Bottino, G. Capannelli, and A. Comite, “Preparation and characterization of novel porous PVDF-Zr02 composite membranes,” vol. 146, pp. 35–40, 2002.

[18] B. Moermans, W. De Beuckelaer, I. F. J. Vankelecom, R. Ravishankar, J. A. Martens, and P. A. Jacobs, “Incorporation of nano-sized zeolites in membranes,” *Chem. Commun.*, no. 24, pp. 2467–2468, 2000.

[19] P. S. Goh and A. F. Ismail, “Flat-Sheet Membrane for Power Generation and Desalination Based on Salinity Gradient,” in *Membrane-Based Salinity Gradient Processes for Water Treatment and Power Generation*, Elsevier, 2018, pp. 155–174.

[20] J. Wei, X. Jian, C. Wu, S. Zhang, and C. Yan, “Influence of polymer structure on thermal stability of composite membranes,” vol. 256, pp. 116–121, 2005.

[21] I. Kim, J. Jegal, and K. Lee, “Effect of aqueous and organic solutions on the performance of polyamide thin-film-composite nanofiltration membranes,” *J. Polym. Sci. Part B Polym. Phys.*, vol. 40, no. 19, pp. 2151–2163, 2002.

[22] S. Verissimo, K.-V. Peinemann, and J. Bordado, “Thin-film composite hollow fiber membranes: an optimized manufacturing method,” *J. Memb. Sci.*, vol. 264, no. 1–2, pp. 48–55, 2005.

[23] A. P. Korikov, P. B. Kosaraju, and K. K. Sirkar, “Interfacially polymerized hydrophilic microporous thin film composite membranes on porous polypropylene hollow fibers and flat films,” *J. Memb. Sci.*, vol. 279, no. 1–2, pp. 588–600, 2006.

[24] B. Khorshidi, T. Thundat, B. A. Fleck, and M. Sadrzadeh, “Thin film composite polyamide membranes: parametric study on the influence of synthesis conditions,” *RSC Adv.*, vol. 5, no. 68, pp. 54985–54997, 2015.

[25] K. P. Lee, T. C. Arnot, and D. Mattia, “A review of reverse osmosis membrane materials for desalination—development to date and future potential,” *J. Memb. Sci.*, vol. 370, no. 1–2, pp. 1–22, 2011.

[26] N. Bui, M. Laura, E. M. V Hoek, and J. R. Mccutcheon, “Electrospun nanofiber supported thin film composite membranes for engineered osmosis,” *J. Memb. Sci.*, vol. 385–386, pp. 10–19, 2011.

[27] J. Jegal, S. G. Min, and K. Lee, “Factors affecting the interfacial polymerization of polyamide active layers for the formation of polyamide composite membranes,” *J. Appl. Polym. Sci.*, vol. 86, no. 11, pp. 2781–2787, 2002.

[28] W. Xie, G. M. Geise, B. D. Freeman, H.-S. Lee, G. Byun, and J. E. McGrath, “Polyamide interfacial composite membranes prepared from m-phenylene diamine, trimesoyl chloride and a new disulfonated diamine,” *J. Memb. Sci.*, vol.

403, pp. 152–161, 2012.

[29] I. C. Escobar, E. M. Hoek, C. J. Gabelich, and F. A. DiGiano, “Committee report: recent advances and research needs in membrane fouling,” *Am. Water Work. Assoc. J.*, vol. 97, no. 8, p. 79, 2005.

[30] T.-H. Bae and T.-M. Tak, “Effect of TiO2 nanoparticles on fouling mitigation of ultrafiltration membranes for activated sludge filtration,” *J. Memb. Sci.*, vol. 249, no. 1–2, pp. 1–8, 2005.

[31] J.-H. Li, Y.-Y. Xu, L.-P. Zhu, J.-H. Wang, and C.-H. Du, “Fabrication and characterization of a novel TiO2 nanoparticle self-assembly membrane with improved fouling resistance,” *J. Memb. Sci.*, vol. 326, no. 2, pp. 659–666, 2009.

[32] A. Dror-Ehre, A. Adin, and H. Mamane, “Control of membrane biofouling by silver nanoparticles using Pseudomonas aeruginosa as a model bacterium,” *Desalin. Water Treat.*, vol. 48, no. 1–3, pp. 130–137, 2012.

[33] L. Yan, Y. S. Li, C. B. Xiang, and S. Xianda, “Effect of nano-sized Al2O3-particle addition on PVDF ultrafiltration membrane performance,” *J. Memb. Sci.*, vol. 276, no. 1–2, pp. 162–167, 2006.

[34] A. A. Adesina, “Industrial exploitation of photocatalysis: progress, perspectives and prospects,” *Catal. Surv. from Asia*, vol. 8, no. 4, pp. 265–273, 2004.

[35] K. Kabra, R. Chaudhary, and R. L. Sawhney, “Treatment of hazardous organic and inorganic compounds through aqueous-phase photocatalysis: a review,” *Ind. Eng. Chem. Res.*, vol. 43, no. 24, pp. 7683–7696, 2004.

[36] I. A. Azeez, “Facile preparation of antiadhesive and biocidal reverse osmosis membranes using a single coating for efficient water purification,” 2019.

[37] L. Jin, Z. Wang, S. Zheng, and B. Mi, “Polyamide-crosslinked graphene oxide membrane for forward osmosis,” *J. Memb. Sci.*, vol. 545, pp. 11–18, 2018.

[38] F. Perreault, A. F. De Faria, and M. Elimelech, “Environmental applications of graphene-based nanomaterials,” *Chem. Soc. Rev.*, vol. 44, no. 16, pp. 5861–5896, 2015.

[39] Q. Nan, P. Li, and B. Cao, “Fabrication of positively charged nanofiltration membrane via the layer-by-layer assembly of graphene oxide and polyethylenimine for desalination,” *Appl. Surf. Sci.*, vol. 387, pp. 521–528, 2016.

[40] M. J. Park *et al.*, “Graphene oxide incorporated polysulfone substrate for the fabrication of flat-sheet thin-film composite forward osmosis membranes,” *J. Memb. Sci.*, vol. 493, pp. 496–507, 2015.

[41] H.- Rez, C. Republic, S. Bakardjieva, T. M. Grygar, and M. Kormunda, “TiO 2 - graphene oxide nanocomposite as advanced photocatalytic materials,” no. May 2014, 2013.

[42] S. Qiu, L. Wu, G. Shi, L. Zhang, H. Chen, and C. Gao, “Preparation and pervaporation property of chitosan membrane with functionalized multiwalled carbon nanotubes,” *Ind. Eng. Chem. Res.*, vol. 49, no. 22, pp. 11667–11675, 2010.

[43] L. Huang and J. R. McCutcheon, “Impact of support layer pore size on performance of thin film composite membranes for forward osmosis,” *J. Memb.*

Sci., vol. 483, pp. 25–33, 2015.

[44] A. Giwa, N. Akther, V. Dufour, and S. W. Hasan, "A critical review on recent polymeric and nano-enhanced membranes for reverse osmosis," *RSC Adv.*, vol. 6, no. 10, pp. 8134–8163, 2016.

[45] R. Bi, Q. Zhang, R. Zhang, Y. Su, and Z. Jiang, "Thin fi lm nanocomposite membranes incorporated with graphene quantum dots for high fl ux and antifouling property," *J. Memb. Sci.*, vol. 553, no. January, pp. 17–24, 2018.

[46] J. Yin, G. Zhu, and B. Deng, "Graphene oxide (GO) enhanced polyamide (PA) thin- fi lm nanocomposite (TFN) membrane for water puri fi cation," vol. 379, pp. 93–101, 2016.

[47] D. Pandey, R. Reifenberger, and R. Piner, "Scanning probe microscopy study of exfoliated oxidized graphene sheets," *Surf. Sci.*, vol. 602, no. 9, pp. 1607–1613, 2008.

[48] H.-P. Boehm, A. Clauss, and U. Hofmann, "Graphite oxide and its membrane properties," *J. Chim. Phys.*, vol. 58, pp. 141–147, 1961.

[49] S. Jalali, A. R. Mehrabadi, J. Shayegan, M. Mirabi, and S. S. Madaeni, "Flux enhancement of thin-film composite membrane by graphene oxide incorporation," pp. 377–382, 2019.

[50] W. Yang, Y. Li, and Y. Lee, "Synthesis of r-GO/TiO2 composites via the UV-assisted photocatalytic reduction of graphene oxide," *Appl. Surf. Sci.*, 2016.

[51] W. Zhao, H. Liu, N. Meng, M. Jian, H. Wang, and X. Zhang, "Graphene oxide

incorporated thin film nanocomposite membrane at low concentration monomers," *J. Memb. Sci.*, vol. 565, pp. 380–389, 2018.

[52] S. Zhou *et al.*, "Film structure of epitaxial graphene oxide on SiC: insight on the relationship between interlayer spacing, water content, and intralayer structure," *Adv. Mater. Interfaces*, vol. 1, no. 3, p. 1300106, 2014.

[53] S. Zheng, Q. Tu, J. J. Urban, S. Li, and B. Mi, "Swelling of graphene oxide membranes in aqueous solution: characterization of interlayer spacing and insight into water transport mechanisms," *ACS Nano*, vol. 11, no. 6, pp. 6440–6450, 2017.

[54] S. Bano, A. Mahmood, S.-J. Kim, and K.-H. Lee, "Graphene oxide modified polyamide nanofiltration membrane with improved flux and antifouling properties," *J. Mater. Chem. A*, vol. 3, no. 5, pp. 2065–2071, 2015.

[55] D. Emadzadeh, W. J. Lau, T. Matsuura, M. Rahbari-Sisakht, and A. F. Ismail, "A novel thin film composite forward osmosis membrane prepared from PSf–TiO2 nanocomposite substrate for water desalination," *Chem. Eng. J.*, vol. 237, pp. 70–80, 2014.

[56] S. A. Ansari, M. M. Khan, M. O. Ansari, and M. H. Cho, "Silver nanoparticles and defect-induced visible light photocatalytic and photoelectrochemical performance of Ag@ m-TiO2 nanocomposite," *Sol. Energy Mater. Sol. Cells*, vol. 141, pp. 162–170, 2015.

[57] C. Liu, Y. Teng, R. Liu, S. Luo, L. Chen, and Q. Cai, "Fabrication of graphene films on TiO 2 nanotube arrays for photocatalytic application," *Carbon N. Y.*, vol.

49, no. 15, pp. 5312–5320, 2011.

[58] M. Ravisankar, A. T. Reghunath, K. Sathianandan, and V. P. N. Nampoori, “Effect of dissolved NaCl, MgCl 2, and Na 2 SO 4 in seawater on the optical attenuation in the region from 430 to 630 nm,” *Appl. Opt.*, vol. 27, no. 18, pp. 3887–3894, 1988.

[59] Q. T. Ain, S. H. Haq, A. Alshammari, M. A. Al-Mutlaq, and M. N. Anjum, “The systemic effect of PEG-nGO-induced oxidative stress in vivo in a rodent model,” *Beilstein J. Nanotechnol.*, vol. 10, no. 1, pp. 901–911, 2019.

[60] M. Sharon, F. Modi, and M. Sharon, “Titania based nanocomposites as a photocatalyst: a review,” *AIMS Mater. Sci.*, vol. 3, no. 3, pp. 1236–1254, 2016.

[61] J.-F. Li, Z.-L. Xu, H. Yang, L.-Y. Yu, and M. Liu, “Effect of TiO2 nanoparticles on the surface morphology and performance of microporous PES membrane,” *Appl. Surf. Sci.*, vol. 255, no. 9, pp. 4725–4732, 2009.

[62] Y. Min, K. Zhang, W. Zhao, F. Zheng, Y. Chen, and Y. Zhang, “Enhanced chemical interaction between TiO2 and graphene oxide for photocatalytic decolorization of methylene blue,” *Chem. Eng. J.*, vol. 193, pp. 203–210, 2012.

[63] P. K. Dubey, P. Tripathi, R. S. Tiwari, A. S. K. Sinha, and O. N. Srivastava, “Synthesis of reduced graphene oxide–TiO2 nanoparticle composite systems and its application in hydrogen production,” *Int. J. Hydrogen Energy*, vol. 39, no. 29, pp. 16282–16292, 2014.

[64] H. Sun, S. Liu, S. Liu, and S. Wang, “A comparative study of reduced graphene

oxide modified TiO2, ZnO and Ta2O5 in visible light photocatalytic/photochemical oxidation of methylene blue," *Appl. Catal. B Environ.*, vol. 146, pp. 162–168, 2014.

[65] W. Li, R. Liang, A. Hu, Z. Huang, and Y. Zhou, "Generation of oxygen vacancies in visible light activated one-dimensional iodine TiO2 photocatalysts," *RSC Adv.*, vol. 4, Aug. 2014.

[66] C. Patomnetikul, S. Thongtem, and S. Narksitipan, "Characterization of GO and TiO2-GO composites prepared by using microwave technique," in *International Conference on Experimental Mechanics 2013 and Twelfth Asian Conference on Experimental Mechanics*, 2014, vol. 9234, p. 923406.

[67] K. Alireza and M. G. Ali, *Nanostructured titanium dioxide materials: Properties, preparation and applications*. World scientific, 2011.

[68] Q. Zhang *et al.*, "Structure and photocatalytic properties of TiO 2-graphene oxide intercalated composite," *Chinese Sci. Bull.*, vol. 56, no. 3, pp. 331–339, 2011.

[69] N. R. Khalid, E. Ahmed, Z. Hong, L. Sana, and M. Ahmed, "Enhanced photocatalytic activity of graphene–TiO2 composite under visible light irradiation," *Curr. Appl. Phys.*, vol. 13, no. 4, pp. 659–663, 2013.

[70] T.-D. Nguyen-Phan *et al.*, "The role of graphene oxide content on the adsorption-enhanced photocatalysis of titanium dioxide/graphene oxide composites," *Chem. Eng. J.*, vol. 170, no. 1, pp. 226–232, 2011.

[71] J. Chen, B. Yao, C. Li, and G. Shi, "An improved Hummers method for eco-

friendly synthesis of graphene oxide," *Carbon N. Y.*, vol. 64, pp. 225–229, 2013.

[72] M. Safarpour, A. Khataee, and V. Vatanpour, "Preparation of a novel PVDF ultrafiltration membrane modified with reduced graphene oxide/TiO2 nanocomposite with enhanced hydrophilicity and antifouling properties. 53," *Ind. Eng. Chem. Res.*, vol. 53, pp. 13370–13382, 2014.

[73] W. Low and V. Boonamnuayvitaya, "A study of photocatalytic graphene–TiO2 synthesis via peroxo titanic acid refluxed sol," *Mater. Res. Bull.*, vol. 48, no. 8, pp. 2809–2816, 2013.

[74] H. Zhang, X. Lv, Y. Li, Y. Wang, and J. Li, "P25-graphene composite as a high performance photocatalyst," *ACS Nano*, vol. 4, no. 1, pp. 380–386, 2010.

[75] H. Gao *et al.*, "Controllable O2•− oxidization graphene in TiO2/graphene composite and its effect on photocatalytic hydrogen evolution," *Int. J. Hydrogen Energy*, vol. 38, no. 29, pp. 13110–13116, 2013.

[76] K. D. Kumar, G. P. Kumar, and K. S. Reddy, "Rapid microwave synthesis of reduced graphene oxide-supported TiO2 nanostructures as high performance photocatalyst," *Mater. Today Proc.*, vol. 2, no. 4–5, pp. 3736–3742, 2015.

[77] J. Pouilleau, D. Devilliers, H. Groult, and P. Marcus, "Surface study of a titanium-based ceramic electrode material by X-ray photoelectron spectroscopy," *J. Mater. Sci.*, vol. 32, no. 21, pp. 5645–5651, 1997.

[78] Z. Qianqian, B. Tang, and H. Guoxin, "High photoactive and visible-light responsive graphene/titanate nanotubes photocatalysts: Preparation and

characterization," *J. Hazard. Mater.*, vol. 198, pp. 78–86, 2011.

[79] J. Yang, M. Wu, F. Chen, Z. Fei, and M. Zhong, "Preparation, characterization, and supercritical carbon dioxide foaming of polystyrene/graphene oxide composites," *J. Supercrit. Fluids*, vol. 56, no. 2, pp. 201–207, 2011.

[80] M. Kumar, Z. Gholamvand, A. Morrissey, K. Nolan, M. Ulbricht, and J. Lawler, "Preparation and characterization of low fouling novel hybrid ultrafiltration membranes based on the blends of GO− TiO2 nanocomposite and polysulfone for humic acid removal," *J. Memb. Sci.*, vol. 506, pp. 38–49, 2016.

[81] M. Safarpour, A. Khataee, and V. Vatanpour, "Thin fi lm nanocomposite reverse osmosis membrane modi fi ed by reduced graphene oxide / TiO 2 with improved desalination performance," vol. 489, pp. 43–54, 2015.

[82] Y. Xie, X. Z. Ã, Y. Chen, Q. Zhao, and Q. Yuan, "Preparation and characterization of porous C-modified anatase titania films with visible light catalytic activity," vol. 180, pp. 3576–3582, 2007.

[83] C. Chen *et al.*, "Journal of Molecular Catalysis A : Chemical Preparation , characterization and visible-light activity of carbon modified TiO 2 with two kinds of carbonaceous species," vol. 314, pp. 35–41, 2009.

[84] D. Yang *et al.*, "Chemical analysis of graphene oxide films after heat and chemical treatments by X-ray photoelectron and Micro-Raman spectroscopy," *Carbon N. Y.*, vol. 47, no. 1, pp. 145–152, 2009.

[85] S. Yumitori, "Correlation of C 1s chemical state intensities with the O 1s intensity

in the XPS analysis of anodically oxidized glass-like carbon samples," vol. 5, pp. 139–146, 2000.

[86] J. Sha, N. Zhao, and E. Liu, "In situ synthesis of ultrathin 2-D TiO 2 with high energy facets on graphene oxide for enhancing photocatalytic activity," *Carbon N. Y.*, vol. 68, pp. 352–359, 2013.

[87] D. C. Marcano *et al.*, "Improved Synthesis of Graphene Oxide," vol. 4, no. 8.

[88] S. S. Æ. B. Smitha, Æ. S. Mayor, and B. P. Æ. T. M. Aminabhavi, "Gas permeation properties of polyamide membrane prepared by interfacial polymerization," pp. 9392–9401, 2007.

[89] C. Y. Tang, Y. Kwon, and J. O. Leckie, "Probing the nano- and micro-scales of reverse osmosis membranes — A comprehensive characterization of physiochemical properties of uncoated and coated membranes by XPS , TEM , ATR-FTIR , and streaming potential measurements," vol. 287, pp. 146–156, 2007.

[90] X. Zhou, P. Zhang, X. Jiang, and G. Rao, "Vibrational Spectroscopy Influence of maleic anhydride grafted polypropylene on the miscibility of polypropylene / polyamide-6 blends using ATR-FTIR mapping," vol. 49, pp. 17–21, 2009.

[91] K. Alamelu, V. Raja, L. Shiamala, and B. M. J. Ali, "Biphasic TiO 2 nanoparticles decorated graphene nanosheets for visible light driven photocatalytic degradation of organic dyes Applied Surface Science Biphasic TiO 2 nanoparticles decorated graphene nanosheets for visible light driven photocatalytic degra," *Appl. Surf. Sci.*, vol. 430, no. May, pp. 145–154, 2017.

[92] B. Rajaeian, A. Rahimpour, M. O. Tade, and S. Liu, “Fabrication and characterization of polyamide thin fi lm nanocomposite (TFN) nano fi ltration membrane impregnated with TiO 2 nanoparticles,” vol. 313, pp. 176–188, 2013.

[93] L. Palacio, J. I. Calvo, P. Prádanos, A. Hernández, P. Väisänen, and M. Nyström, “Contact angles and external protein adsorption onto UF membranes,” *J. Memb. Sci.*, vol. 152, no. 2, pp. 189–201, 1999.

[94] L. Zhu, M. Wu, B. Van Der Bruggen, L. Lei, and L. Zhu, “Separation and Puri fi cation Technology E ff ect of TiO 2 content on the properties of polysulfone nano fi ltration membranes modi fi ed with a layer of TiO 2 – graphene oxide,” vol. 242, no. December 2019, 2020.

[95] M. Y. Kiriukhin and K. D. Collins, “Dynamic hydration numbers for biologically important ions,” *Biophys. Chem.*, vol. 99, no. 2, pp. 155–168, 2002.

[96] P. V Kumar, N. M. Bardhan, S. Tongay, J. Wu, A. M. Belcher, and J. C. Grossman, “Scalable enhancement of graphene oxide properties by thermally driven phase transformation,” *Nat. Chem.*, vol. 6, no. 2, p. 151, 2014.

Vitae

Name : Anwar Qasem Al Gamal

Nationality : Yemeni

Date of Birth : 1/1/1991

Email : anwaraljamal2@gmail.com

Telephone : 00966533591275

Present Address : Ad-Daleel, Al Makhadir, Ibb 1120, Yemen

Academic Background : M.S Mechanical Engineering (April 2021)

KFUPM, Dhahran, Saudi Arabia

B.Sc. Mechanical Engineering (January 2018)

KFUPM, Dhahran, Saudi Arabia

Journal Publication : Al-Gamal, Anwar Q., Wail S. Falath, and Tawfik A. Saleh. "Enhanced efficiency of polyamide membranes by incorporating TiO_2 - Graphene oxide for water purification." Journal of Molecular Liquids 323 (2021): 114922.